National Advisory Committee
for Aeronautics
MAILED
NOV 7 1939
To Library, L.M.A.L.

NOV 17 1939

TECHNICAL NOTES

NATIONAL ADVISORY COMMITTEE FOR AERONAUTICS

No. 734

TN 734

PRESSURE-DISTRIBUTION INVESTIGATION OF AN N.A.C.A. 0009 AIRFOIL WITH A 50-PERCENT-CHORD PLAIN FLAP AND THREE TABS

By William G. Street and Milton B. Ames, Jr.
Langley Memorial Aeronautical Laboratory

Transferred to the files of the Langley Memorial Aeronautical Laboratory.

Washington
November 1939

NATIONAL ADVISORY COMMITTEE FOR AERONAUTICS

TECHNICAL NOTE NO. 734

PRESSURE-DISTRIBUTION INVESTIGATION OF AN N.A.C.A. 0009 AIRFOIL WITH A 50-PERCENT-CHORD PLAIN FLAP AND THREE TABS

By William G. Street and Milton B. Ames, Jr.

SUMMARY

Pressure-distribution tests of an N.A.C.A. 0009 airfoil with a 50-percent-chord plain flap and three plain tabs, having chords 10, 20, and 30 percent of the flap chord, were made in the N.A.C.A. 4- by 6-foot vertical tunnel. The tests supplied aerodynamic section data that may be applied to the design of horizontal and vertical tail surfaces.

The results are presented as resultant-pressure diagrams for the airfoil with the flap and the 20-percent-chord tab. Plots are also given of increments of normal-force and hinge-moment coefficients for the airfoil, the flap, and the three tabs. The experimental results and values computed by analytical methods are in good agreement for small flap and tab deflections. The results of the tests indicated that the effectiveness of all three tab sizes in reducing flap hinge moments decreased with increasing flap deflection.

INTRODUCTION

The recent increases in speed and size of airplanes have produced excessive control forces. At the present time, one of the most effective devices for reducing these high control forces is the trailing-edge tab. (See references 1 and 2.) Previous investigations have indicated the effects of such factors as plan form, cut-outs, end plates, elevator nose shape, gap, and balance on the aerodynamic characteristics of some tail surfaces of finite span (references 3 and 4). No available data applicable to tail-surface design, however, give the section aerody-

namic characteristics of a thin airfoil as affected by flaps and tabs. The present investigation was therefore undertaken to supply information that would be applicable for use in aerodynamic and structural design of tail surfaces with tabs.

The tests consisted of pressure-distribution measurements over one section of an N.A.C.A. 0009 airfoil with a 50-percent-chord plain flap and with plain tabs 10, 20, and 30 percent of the flap chord. From the data obtained, normal-force and pitching-moment coefficients were calculated for the airfoil section complete with the flap and the various tabs. In addition, normal-force and hinge-moment coefficients were calculated for the flap with the different tabs and for the tabs alone.

APPARATUS AND TESTS

Model and Test Installation

The tests were conducted in the N.A.C.A. 4- by 6-foot vertical wind tunnel. This tunnel, originally a 5-foot open-jet vertical wind tunnel (reference 5), has recently been modified by the substitution of a 4- by 6-foot closed test chamber and a new entrance cone. A diagram of the test chamber and the model is shown in figure 1.

The 3- by 4-foot model was made of laminated mahogany to the N.A.C.A. 0009 profile. The model was constructed with a plain flap having a chord 50 percent of the wing chord (0.50c) and three serially hinged plain tabs, having chords of 10, 20, and 30 percent of the flap chord, as shown in figure 2. During the tests, all flap and tab gaps were sealed with plasticine and cellulose tape to prevent air leakage.

A single row of pressure orifices was built into the upper and the lower surfaces of the main airfoil, the flap, and the tabs at the midspan. The orifices were located on the model as shown in figure 3.

The model, when mounted in the tunnel, completely spanned the test section. With this type of installation, approximate two-dimensional flow is obtained and the section characteristics of the airfoil can be determined.

The model was attached to the balance frame by torque tubes, which extended through the sides of the tunnel. The angle of attack was set from outside the tunnel by rotating the torque tubes with an electric drive.

The tubes from the pressure orifices were brought out of the model at one end through the torque tube and the tunnel wall and were connected to a photographically recording multiple-tube manometer.

Tests

The tests were conducted at an effective Reynolds Number of 3,410,000. (Effective Reynolds Number = test Reynolds Number × turbulence factor. The turbulence factor of the 4- by 6-foot vertical tunnel is 1.93.) The average dynamic pressure was 10.8 pounds per square foot, corresponding to an air speed of about 65 miles per hour at standard sea-level conditions.

The tests were run at angles of attack from $-14\frac{1}{2}^\circ$ to $10\frac{1}{2}^\circ$ at intervals of 5°. The model was tested with the 0.50c flap set at angles of 0°, 5°, 10°, 20°, 30°, and 45° down for each of the three tab sizes. Tests were made throughout the entire angle-of-attack range for each flap deflection with tab deflections of 0°, $\pm 10^\circ$, $\pm 20^\circ$, and $\pm 30^\circ$.

RESULTS

Presentation of Data

The results of the distribution of pressures are given in the form of resultant-pressure-increment diagrams, which represent changes in resultant-pressure distribution caused by a change in angle of any one part or any combination of the component parts of the airfoil. All diagrams of resultant pressure or resultant-pressure increment of the airfoil, flap, and tab combination are plotted as pressure coefficients, P, or as ΔP, where

$$P = \frac{p - p_o}{q}$$

and

p is static pressure at a point on the airfoil.

p_o, static pressure in the free air stream.

q, dynamic pressure of the free air stream.

In order to enable the designer to obtain the original resultant-pressure diagram for any condition, resultant-pressure diagrams are given for the basic section (i.e., flap and tab neutral, fig. 4) which, when added to the increment diagrams (figs. 5 to 10) give the desired result.

Because the large quantity of data prohibited the inclusion of the resultant-pressure-increment diagrams for all tab sizes, only the diagrams for the $0.20c_f$ tab, which was considered to be an average size, are presented. Values of angle of attack were also selected to represent the negative angle-of-attack condition, $\alpha = -9\frac{1}{2}^\circ$; the low angle-of-attack condition, $\alpha = 1/2^\circ$; and the positive angle-of-attack condition, $\alpha = 5\frac{1}{2}^\circ$. The value of $5\frac{1}{2}^\circ$ may seem rather low; but, with such a large-chord flap, the stall occurs at low angles of attack.

The section characteristics of the airfoil, the flap, and the tab, as functions of flap and tab deflection, are also plotted as increments, which were obtained by deducting the basic section coefficients from those for the section with the tab, the flap, or the combination deflected. The characteristics were obtained in each case by mechanical integration of the original plotted pressure diagrams.

Computations were made to determine the section coefficients, which are defined as follows:

$c_n = \frac{n}{q\ c}$, airfoil section normal-force coefficient.

$c_m = \frac{m}{q\ c^2}$, airfoil section pitching-moment coefficient about quarter-chord point of airfoil.

$c_{n_f} = \frac{n_f}{q\ c_f}$, flap section normal-force coefficient.

$c_{h_f} = \frac{h_f}{q\ c_f^2}$, flap section hinge-moment coefficient.

$c_{n_t} = \frac{n_t}{q\ c_t}$, tab section normal-force coefficient.

$c_{h_t} = \frac{h_t}{q\ c_t^2}$, tab section hinge-moment coefficient.

where the forces and moments per unit span are:

n, normal force of airfoil section.

m, pitching moment of airfoil section about the quarter-chord point.

n_f, normal force of flap section.

h_f, hinge moment of flap section.

n_t, normal force of tab section.

h_t, hinge moment of tab section.

and c, chord of basic airfoil with flap and tab neutral.

c_f, flap chord.

c_t, tab chord.

The subscript f refers to the flap with the tab; and the subscript t, to the tab alone.

In figure 11, the integrated coefficients for the basic airfoil are plotted against angle of attack. Curves giving the increments for various tab and flap deflections are presented in figures 12 to 20.

The effect of tab size and deflection on flap section hinge-moment coefficient is shown in figure 21. A comparison of theoretical and experimental airfoil section normal-force and pitching-moment coefficients is given in figure 22.

Precision

Since no air-flow-alinement tests were made in the tunnel for the test set-up used in the investigation, the absolute angle of attack may be slightly in error. In the final data, however, all angles of attack were corrected

for a misalinement of $1/2^{\circ}$, which appeared to be present in the air flow. The relative angles of attack are accurate to within $\pm 0.1^{\circ}$. Tabs and flaps were set to the specified angles to within $\pm 1.0^{\circ}$. Errors in orifice pressures were within ±2 percent except at the nose and the hinge locations on the upper surface, where the variation may be about ±5 percent at high angles of attack. The dynamic-pressure readings were accurate to within ±1.0 percent.

Inasmuch as two-dimensional flow was approximated, the integrated results may be taken as section characteristics. Corrections for tunnel-wall effects (reference 8) were made only to the airfoil section normal-force coefficients c_n. The value of $dc_n/d\alpha$ for the airfoil with flap and tab neutral agrees well with values given in reference 9, but the manner in which the variation of tab and flap angles affects the accuracy of the tunnel correction is not definitely known.

DISCUSSION

Pressure Distribution

The effects of the $0.20c_f$ tab and the $0.50c$ flap deflections on the distribution of resultant-pressure increments or load increments over the main airfoil are shown in figures 4 to 10. These diagrams are useful for application to the structural design of horizontal and vertical tail surfaces having sealed plain flaps with tabs. The diagrams also serve to illustrate some important effects of the action of flaps on the distribution of load increments over the chord of the airfoil.

Figure 5 indicates that, when the tab is deflected, the peak values of the load increments on the tab occur at the tab hinge axis. Deflection of the tab also increases the load on the main airfoil. Similarly, figures 6 to 10 show that, when the flap is deflected, the peak values of the pressure increments on the flap occur at the flap hinge axis. Flap deflections, as in the case of the deflected tab alone, also result in increased loads over the main airfoil.

When the tab and the flap are simultaneously deflected in the same direction, the peak values of the load increments occur at both hinge axes and the resultant pres-

sures act in the same direction. If the tab and the flap are deflected at the same time in opposite directions, then peak values of the pressure increments occur at both hinge axes but the resultant pressures act in opposite directions. (See figs. 6 to 10.)

Several methods have been derived for determining the load distribution over airfoil sections, tabs, and flaps. As a check with the method described in reference 6 for use on plain airfoils, computations were made and the results are plotted with the present experimental results in figure 4. From this comparison, it may be noted that the computed results are almost identical with those obtained from the experiments where the plain airfoil was used. The greatest deviation in the two methods is about 0.2q, which occurs at the nose point of the airfoil.

Calculations of the chordwise load distribution over the airfoil, the flap, and the tab were made by the method described in reference 7, which is an extension of that in reference 6. These computed results are compared with the present experimental results in figures 5, 7, 8, and 9.

In figure 5, the comparison between computed and test results was made for the flap neutral and the tab deflected 30°. A maximum variation of about 0.3q occurred near the leading edge of the airfoil at an angle of attack of $5\frac{1}{2}°$. The other variations were at the hinge axis and did not exceed 0.2q.

For the flap deflected 10° and the tab deflected -30°, 0°, and 30° (fig. 7), the maximum variation of the computed from the experimental results is 0.4q at the airfoil nose. The greatest variation at the hinges is about 0.2q. An excellent correlation was obtained between the computed and the experimental results for 30° and 0° tab deflections. The comparisons made in figures 8 and 9 generally check to within 0.1q.

The comparison shown in figure 8 of computed and experimental load distributions for an angle of attack of 1/2° with the flap deflected 20° and the tab deflected 30°, 0°, and -30° indicates a good agreement for values ahead of the hinge of the flap. Behind the hinge axis, the computed values are about 0.3q lower than the test results. In figure 9, the computed and the experimental results are compared for the flap deflected 30° and the tab deflected 30°, 0°, and -30°. Here the calculated method does not

check so well for high as for low flap deflections.

From the foregoing comparisons, it appears that the methods from references 6 and 7 of determining the load distribution over an airfoil at low flap angles should prove a satisfactory substitute for the experimental method. The discrepancies that occurred may be largely attributed to the effects of the nose radii of the flap and the tabs.

Section Aerodynamic Characteristics

Airfoil characteristics.- The basic airfoil section gave, as expected, linear variation of c_n against angle of attack in the unstalled range. (See fig. 11.) The slope of the normal-force curve, $dc_n/d\alpha$, was found to be 0.095, which agrees with the value given in reference 9, indicating that the tunnel correction was satisfactory for this condition. With a $0.30c_f$ tab, $\alpha = -9\frac{1}{2}^\circ$, $\delta_f = 45^\circ$, and $\delta_t = 30^\circ$ (fig. 18(b)), the maximum value for the increment of airfoil section normal-force coefficient, Δc_n, was 2.32. It is interesting to note that, other conditions remaining the same, deflecting the tab to -30° reduced the value of Δc_n to 1.34, or about 40 percent. For the three sizes of tab tested, a deflection of a tab tended to shift the curve of increment of airfoil section normal-force coefficient against flap deflection parallel to itself, indicating that tab deflection had little effect on the variation of the increment.

For the basic airfoil section, the airfoil section pitching-moment coefficient, c_m, was approximately zero for the range of angles of attack from $-9\frac{1}{2}^\circ$ to $10\frac{1}{2}^\circ$. (See fig. 11.) The value of Δc_m varied almost linearly with flap deflection at a given angle of attack. Although a change in tab deflection gave a corresponding change in Δc_m, the tab effectiveness decreased as the tab deflection was positively or negatively increased.

Flap and tab characteristics.- The increments of flap section normal-force and hinge-moment coefficients varied nearly linearly with flap deflection within the unstalled range of the flap. As would be expected, the flap stalled at successively lower flap deflections as the angle of attack was increased. Deflection of the tab, in general, shifted the curves of Δc_{n_f} and Δc_{h_f} (fig. 13) parallel

to themselves. The magnitude of the shift, however, was not proportional to the tab deflections.

Increments of tab section normal-force and hinge-moment coefficients tended to vary linearly with tab deflection until the tab stalled. Changes in flap angle had little effect on $d\Delta c_{n_t}/d\delta_t$ and $d\Delta c_{h_t}/d\delta_t$ (fig. 14). At given values of α and δ_t, an increase in flap deflection caused increases in Δc_{n_t} and Δc_{h_t}. As the flap deflection was increased, the magnitude of these corresponding increases in Δc_{n_t} and Δc_{h_t} generally became larger. (See fig. 14(b).)

As the c_n of the wing section was increased by increasing the flap deflection, the effectiveness of tabs of all sizes in reducing the flap hinge moment became less, as shown in figure 21. Increase in tab chord at the same c_n and δ_t definitely decreased the flap hinge moments; the decrease in c_{h_f} was not proportional to but decreased with increase in tab chord.

Comparisons with Theory

In figure 22 is given a comparison of curves theoretically calculated, as outlined in reference 1, with some representative curves from the present investigation. Agreement in $dc_n/d\delta_f$ and $dc_m/d\delta_f$ was good for zero tab deflection and up to flap deflections of 10°, after which there was a marked decrease in the experimental slope. The effect of tab deflection on c_n and c_m was about 50 percent of that indicated by theory for 30° tab deflection. Although the values themselves were in poor agreement with the theory, it should be pointed out that both $dc_n/d\delta_f$ and $dc_m/d\delta_f$ were in good agreement up to flap deflections of about 10° for the various tab deflections.

Comparison with the data presented in reference 4 indicates that the rate of change of the normal-force and the flap hinge-moment coefficients with flap deflection are somewhat higher for the present tests than for those reported in reference 4. This condition may be largely attributed to air leakage at the elevator-hinge gap. When the data of this report are applied to tail surfaces of

finite spans and with unsealed elevator-hinge gaps, consideration must therefore be given to these effects

CONCLUDING REMARKS

Aerodynamic section data are made available for an N.A.C.A. 0009 airfoil with a 50-percent-chord plain flap and three plain tabs having chords 10, 20, and 30 percent of the flap chord. The results obtained from the test data show good agreement at low flap and tab deflections with the analytical method for determining chordwise distribution. The tests also indicated that the effectiveness of all three tab sizes in reducing flap hinge moments decreased with increasing flap deflections.

Langley Memorial Aeronautical Laboratory,
National Advisory Committee for Aeronautics,
Langley Field, Va., September 1, 1939.

REFERENCES

1. Wenzinger, Carl J.: Pressure Distribution over an Airfoil Section with a Flap and Tab. T.R. No. 574, N.A.C.A., 1936.

2. Harris, Thomas A.: Reduction of Hinge Moments of Airplane Control Surfaces by Tabs. T.R. No. 528, N.A.C.A., 1935.

3. Silverstein, Abe, and Katzoff, S.: Aerodynamic Characteristics of Horizontal Tail Surfaces. T.N. (to be published), N.A.C.A., 1939.

4. Goett, Harry J., and Reeder, J. P.: Effects of Elevator Nose Shape, Gap, Balance, and Tabs on the Aerodynamic Characteristics of a Horizontal Tail Surface. T.R. No. 675, N.A.C.A., 1939.

5. Wenzinger, Carl J., and Harris, Thomas A.: The Vertical Wind Tunnel of the National Advisory Committee for Aeronautics. T.R. No. 387, N.A.C.A., 1931.

6. Jacobs, Eastman N., and Rhode, R. V.: Airfoil Section Characteristics as Applied to the Prediction of Air Forces and Their Distribution on Wings. T.R. No. 631, N.A.C.A., 1938.

7. Allen, H. Julian: Calculation of the Chordwise Load Distribution over Airfoil Sections with Plain, Split, or Serially Hinged Trailing-Edge Flaps. T.R. No. 634, N.A.C.A., 1938.

8. Wenzinger, Carl J., and Harris, Thomas A.: Wind-Tunnel Investigation of an N.A.C.A. 23012 Airfoil with Various Arrangements of Slotted Flaps. T.R. No. 664, N.A.C.A., 1939.

9. Goett, Harry J., and Bullivant, W. Kenneth: Tests of N.A.C.A. 0009, 0012, and 0018 Airfoils in the Full-Scale Tunnel. T.R. No. 647, N.A.C.A., 1938.

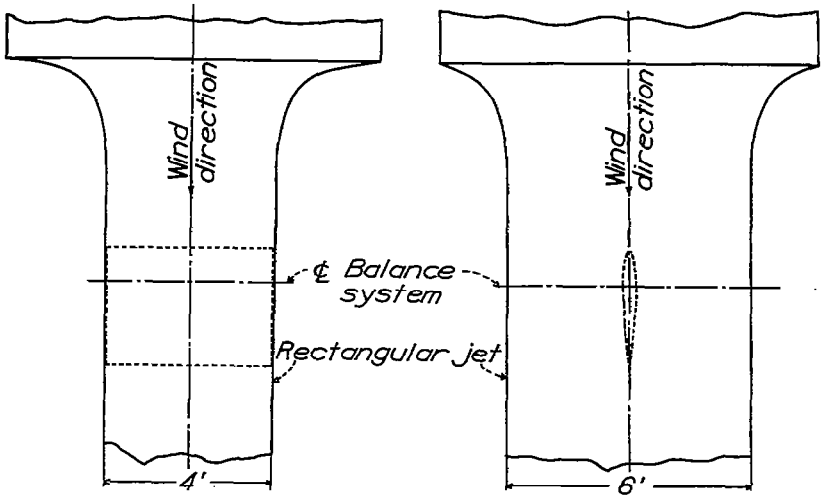

Figure 1.- Model mounted in 4-by 6-foot vertical tunnel.

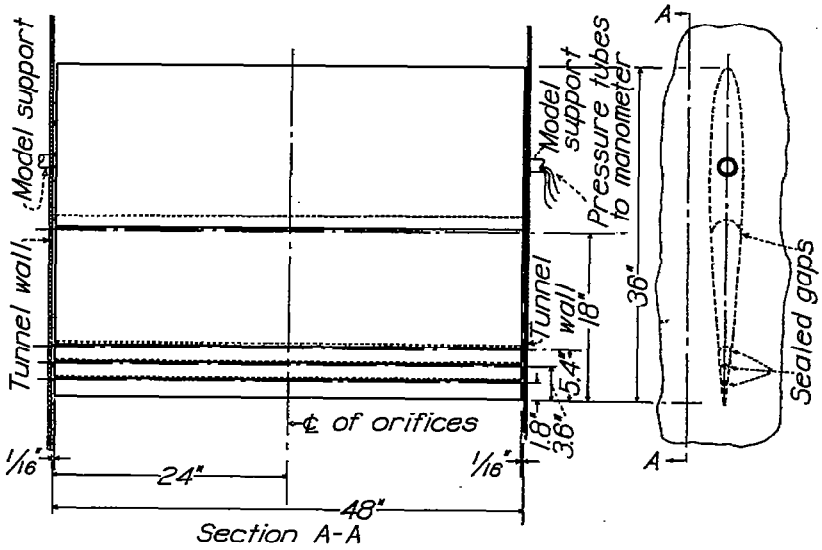

Figure 2.- The N.A.C.A. 0009 pressure-distribution model with 0.50c plain flap and 0.10c_f, 0.20c_f, and 0.30c_f tabs.

Orifice	Location
0	0
1	.625
2	1.25
3	2.5
4	5.0
5	10.0
6	20.0
7	30.0
8	40.0
9	45.0
10	48.25
11	50
12	52.5
13	55
14	60
15	70
16	80
17	82.5
18	84
19	85
20	86.5
21	88
22	89.5
23	90
24	91.5
25	93
26	94.5
27	95
28	96.5
29	98
30	99.5

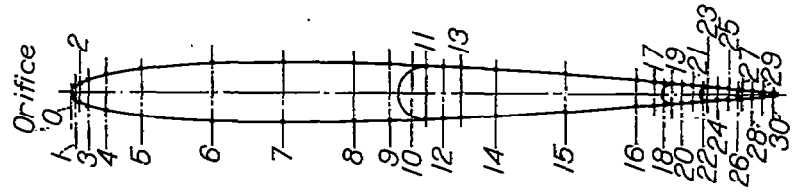

Figure 3.- Chordwise locations of pressure orifices on the N.A.C.A. 0009 airfoil in percent chord.

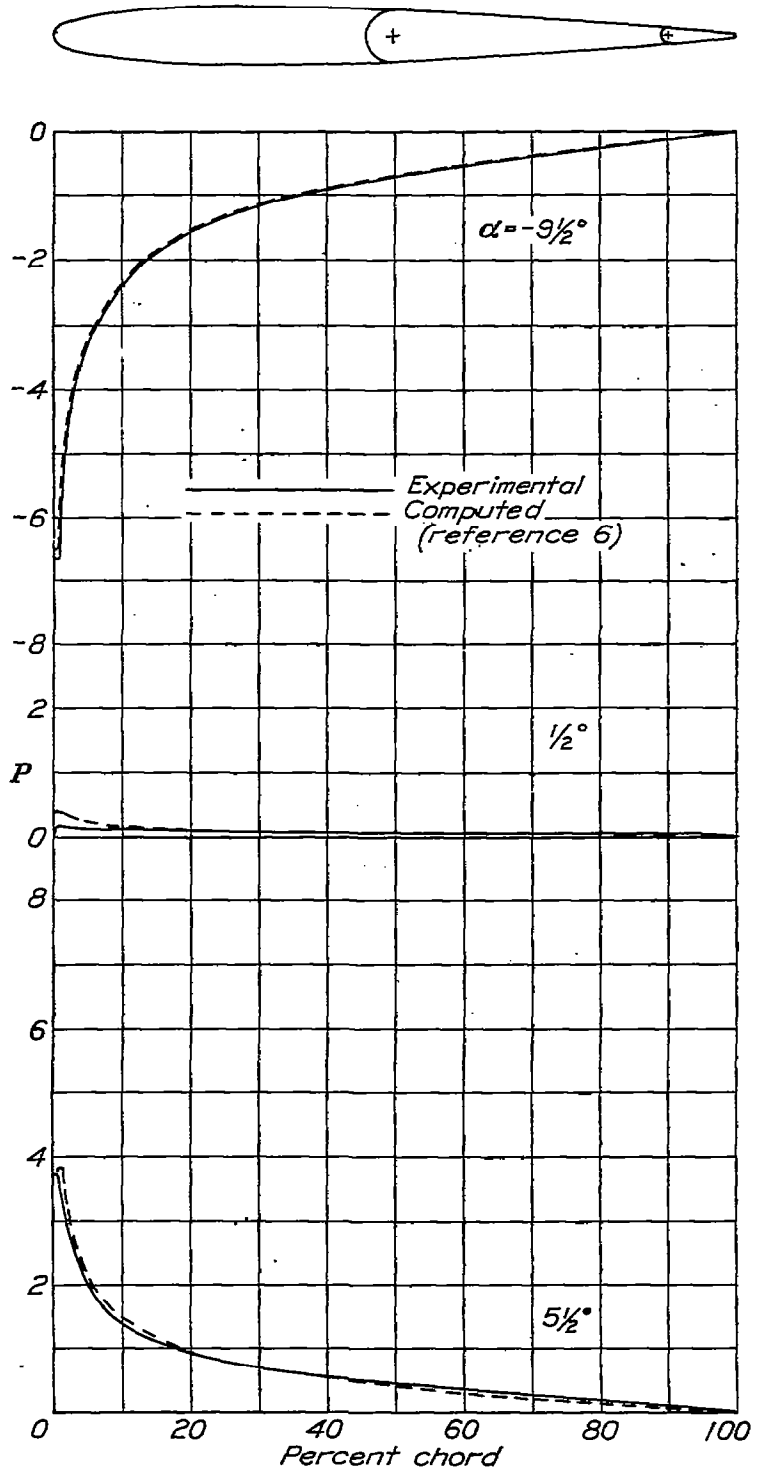

Figure 4.- Distribution of resultant pressure over the N.A.C.A. 0009 airfoil at various angles of attack. Flap and tab neutral.

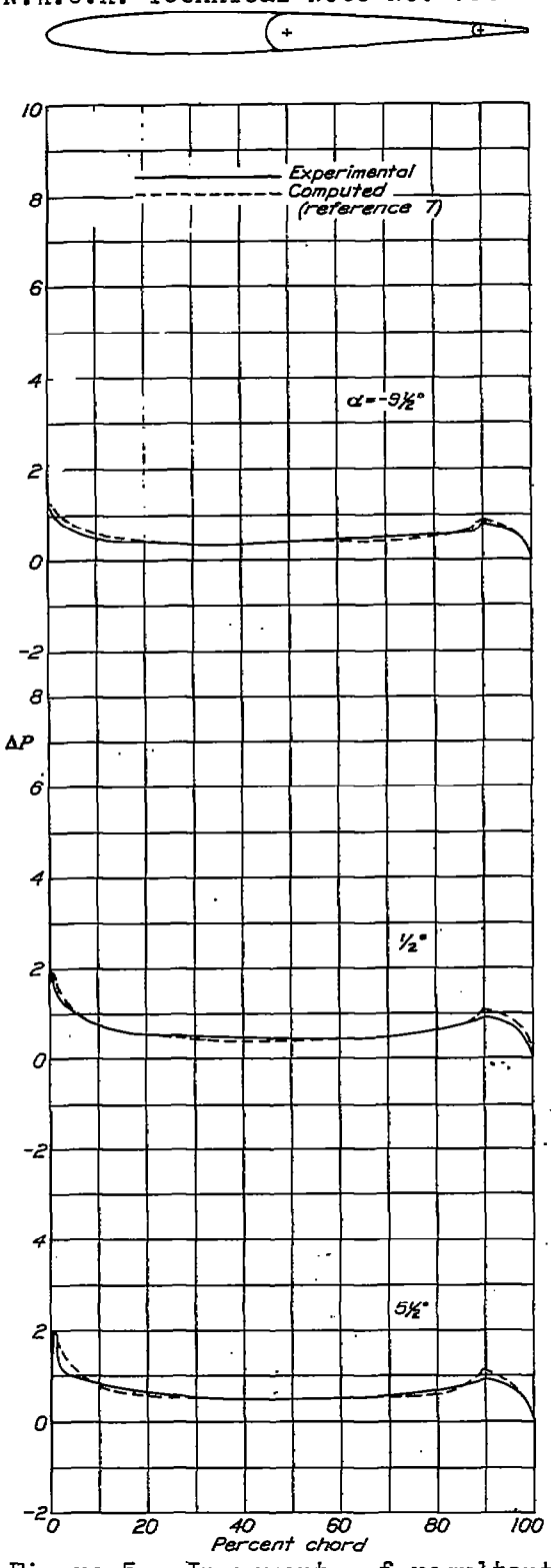

Figure 5.- Increments of resultant pressures for various angles of attack and various deflections of a 0.20c_f tab on a 0.50c plain flap deflected 0°. δ_t,30°.

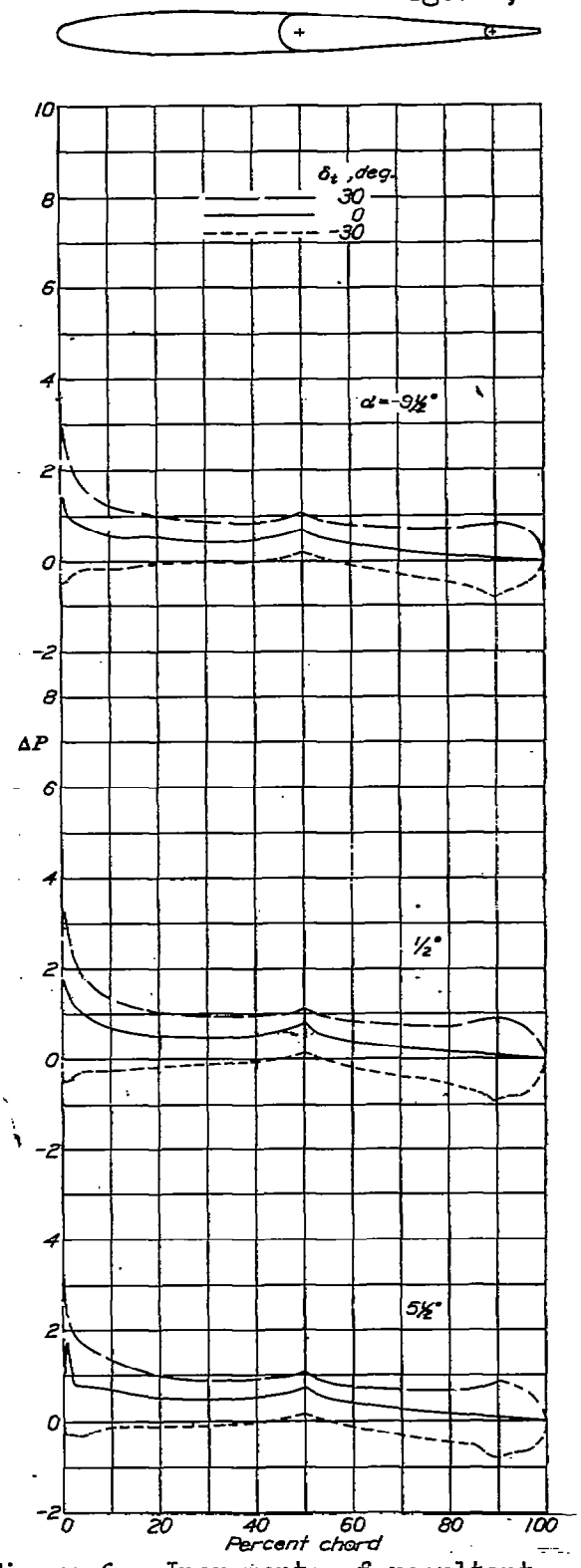

Figure 6.- Increments of resultant pressures for various angles of attack and various deflections of a 0.20c_f tab on a 0.50c plain flap deflected 5°.

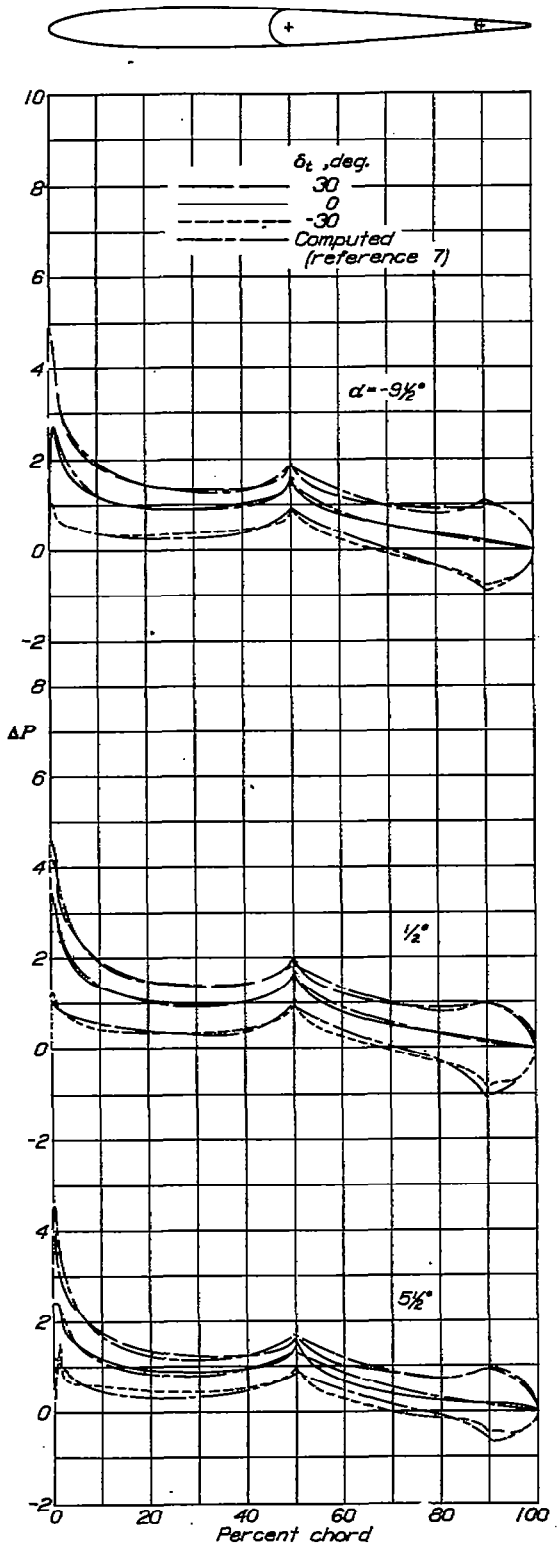

Figure 7.- Increments of resultant pressures for various angles of attack and various deflections of a 0.20c_f tab on a 0.50c plain flap deflected 10°.

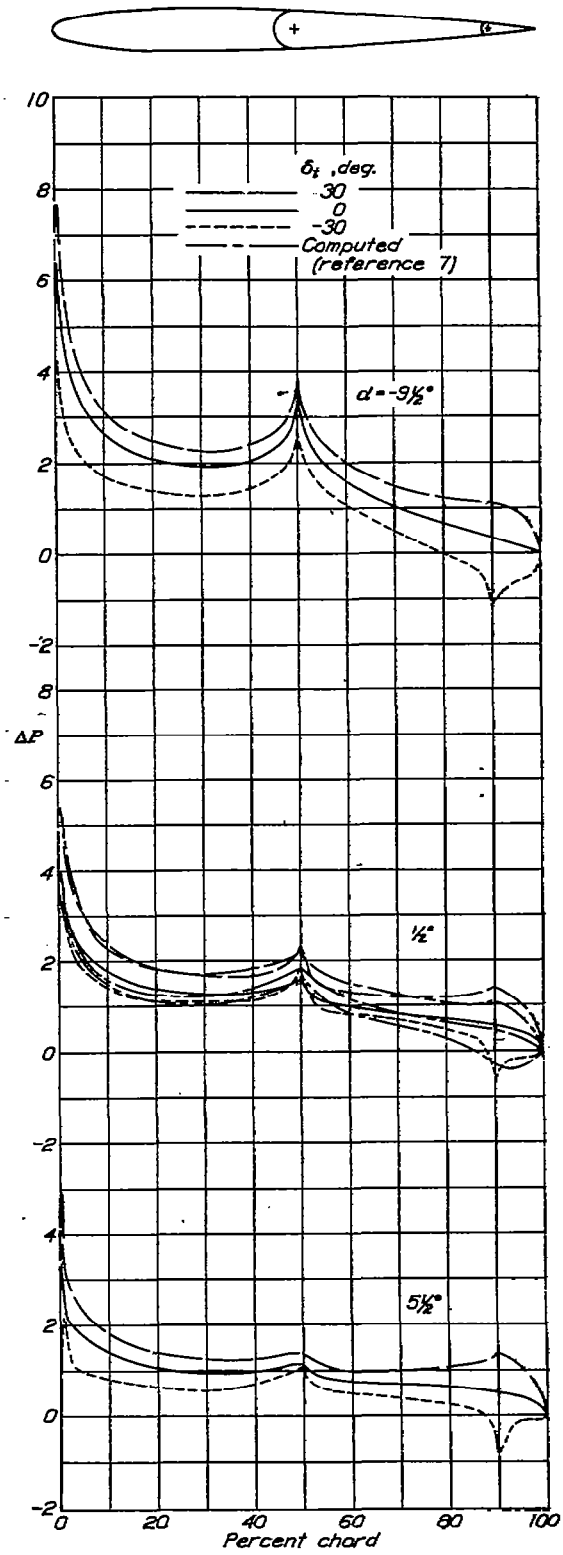

Figure 8.- Increments of resultant pressures for various angles of attack and various deflections of a 0.20c_f tab on a 0.50c plain flap deflected 20°.

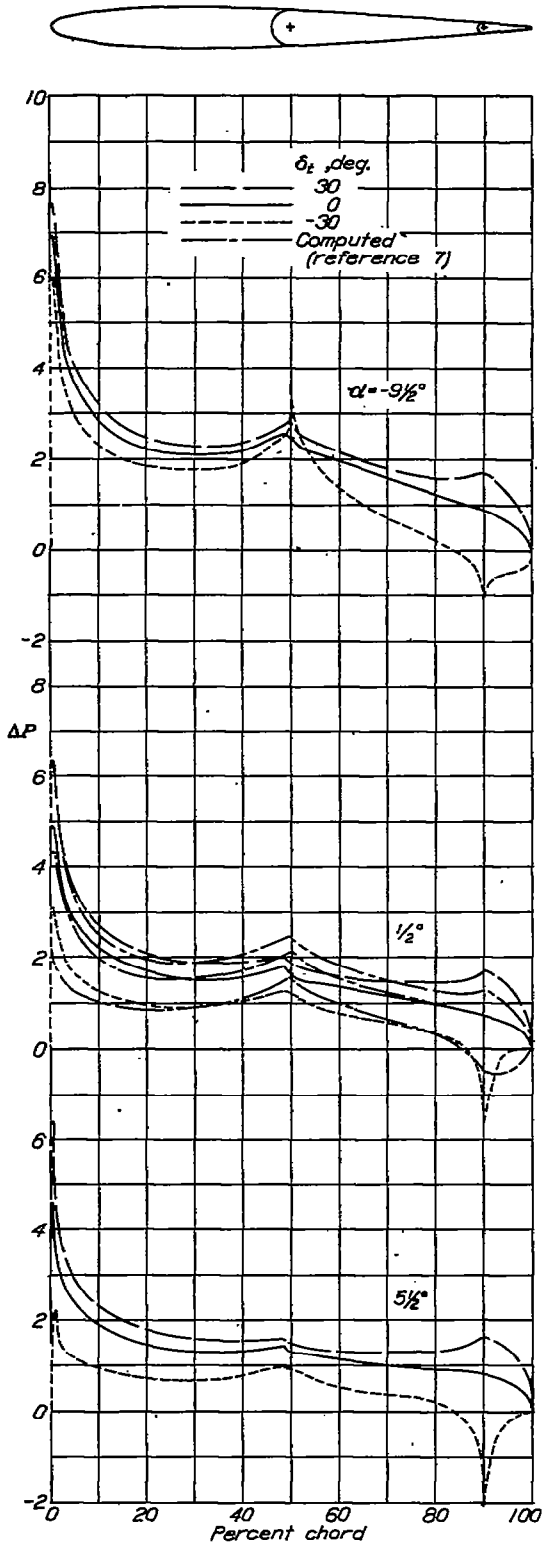

Figure 9.- Increments of resultant pressures for various angles of attack and various deflections of a $0.20c_f$ tab on a 0.50c plain flap deflected 30°.

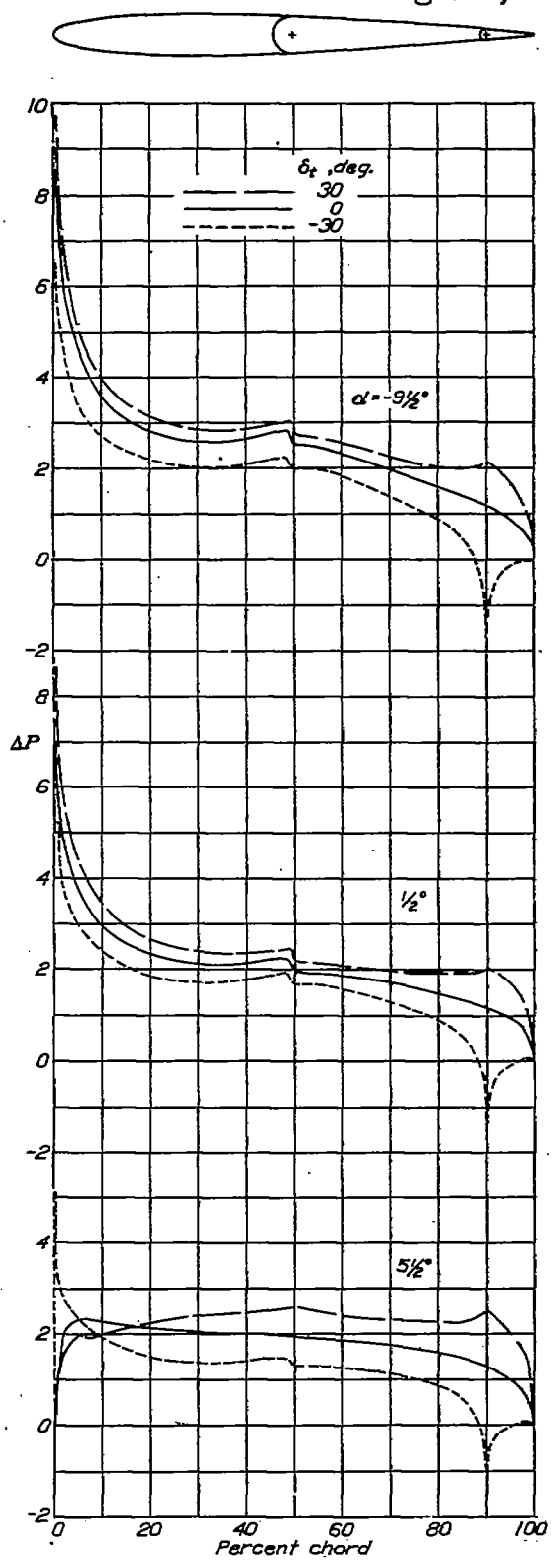

Figure 10.- Increments of resultant pressures for various angles of attack and various deflections of a $0.20c_f$ tab on a 0.50c plain flap deflected 45°.

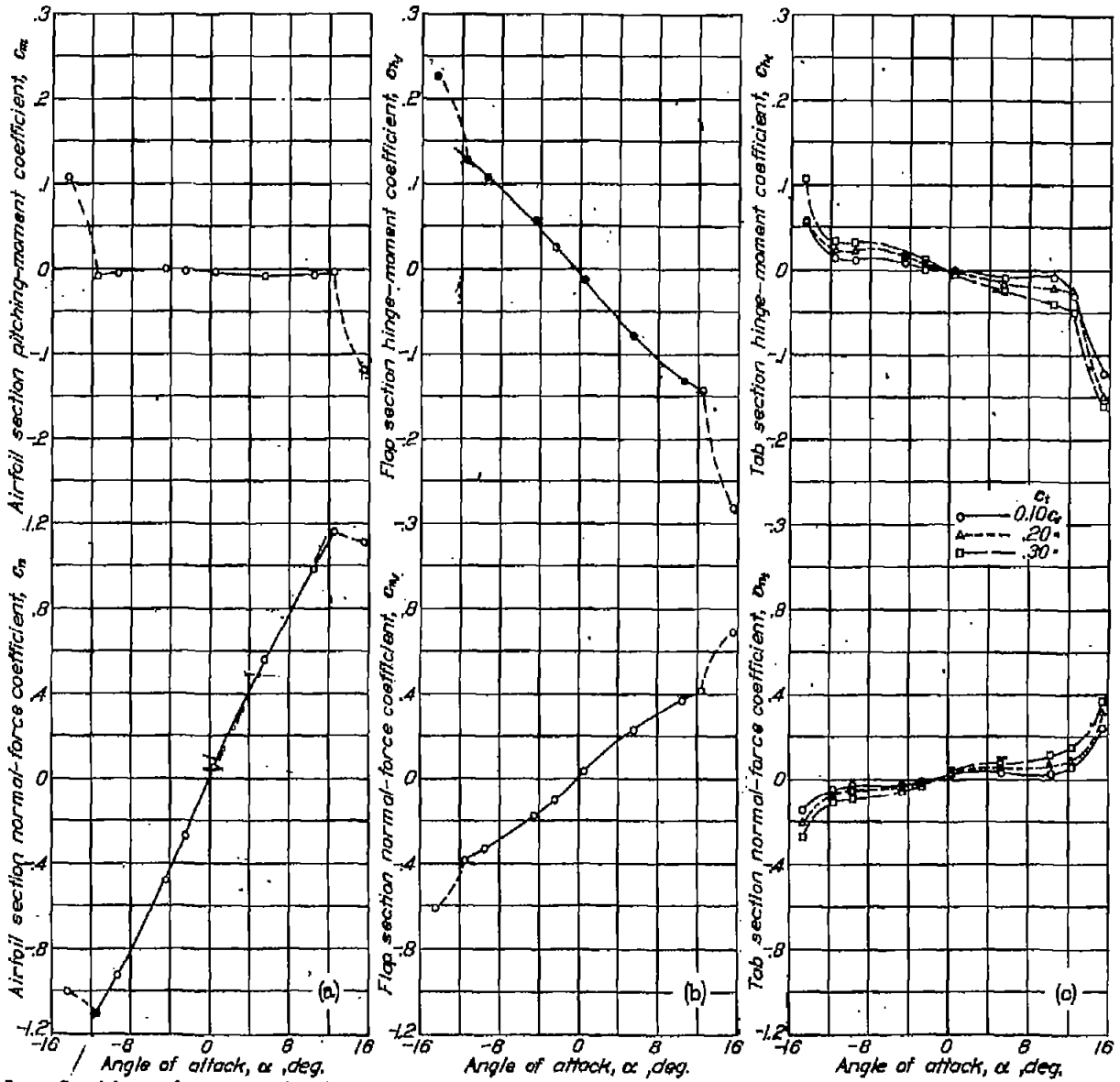

Figure 11.- Section characteristics of basic N.A.C.A. 0009 airfoil with 0.50c plain flap and tabs neutral.

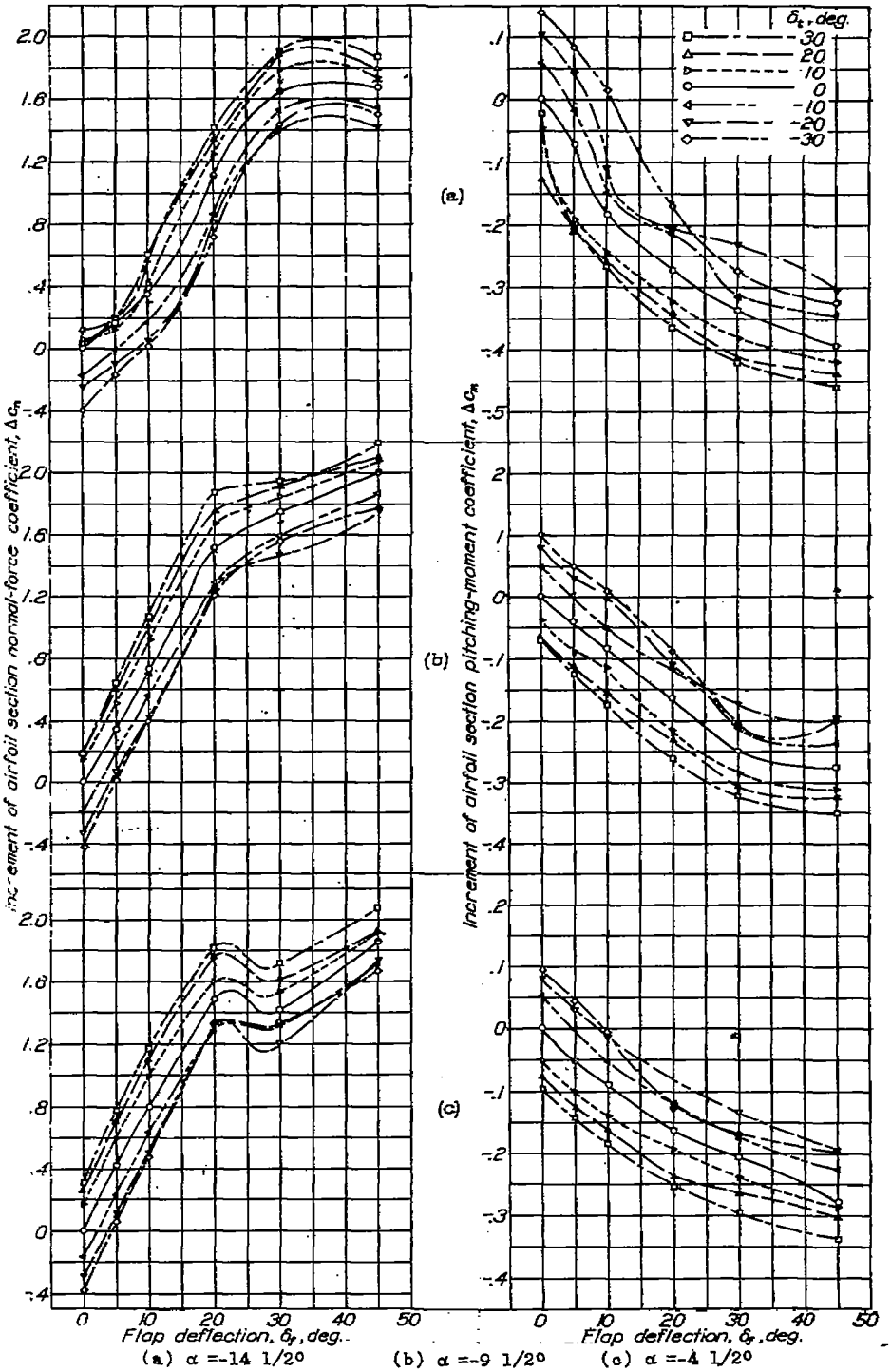

(a) α =-14 1/2° (b) α =-9 1/2° (c) α =-4 1/2°

Figure 12,a to f.- Increments of airfoil section normal-force and pitching-moment coefficients for various deflections of a 0.50c plain flap and a 0.10c_f tab.

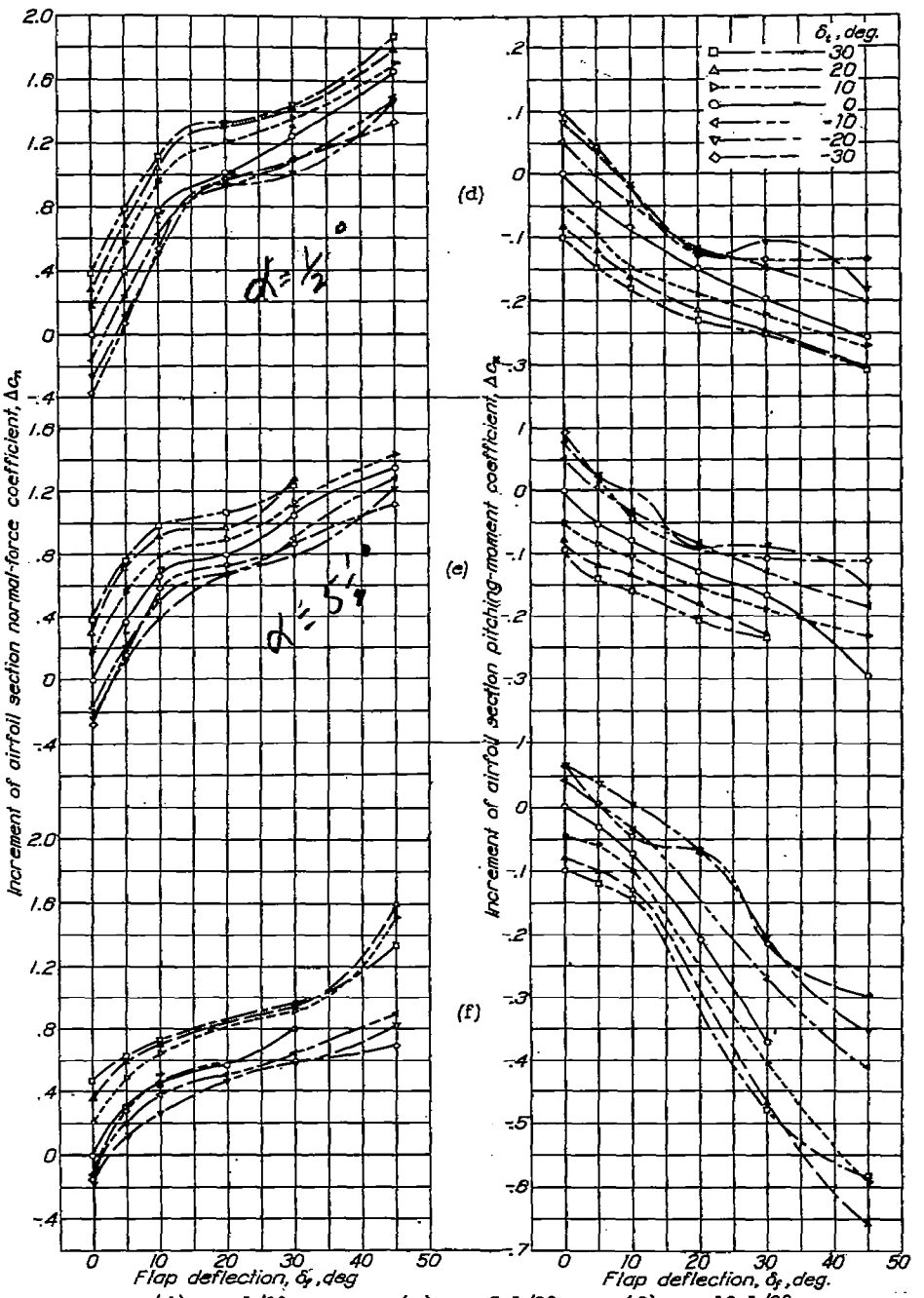

(d) $\alpha = 1/2^\circ$ (e) $\alpha = 5\ 1/2^\circ$ (f) $\alpha = 10\ 1/2^\circ$

Figure 12 concluded.

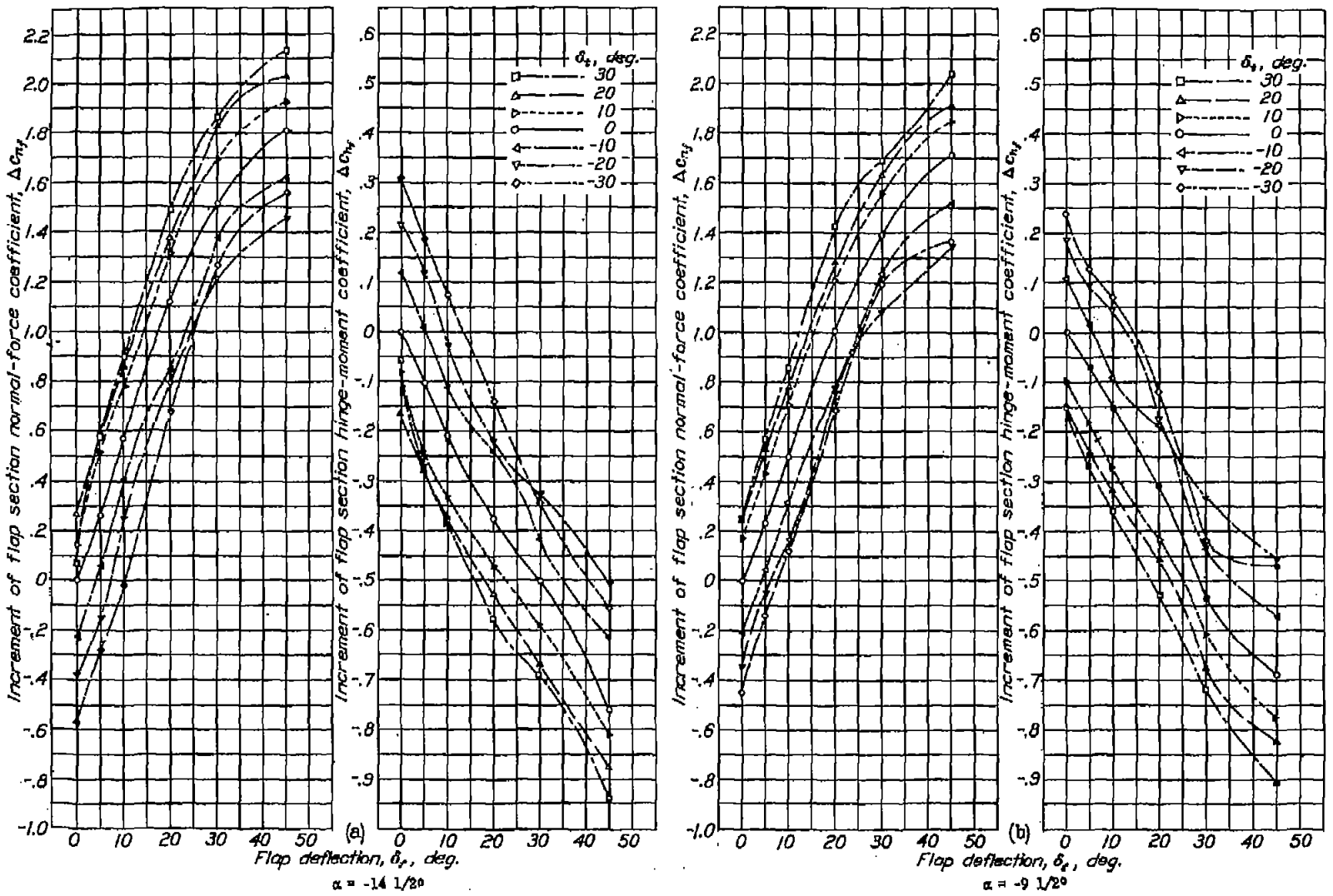

Figure 13,a to f.- Increments of flap section normal-force and hinge-moment coefficients for various deflections of a 0.50c plain flap and a $0.10c_f$ tab.

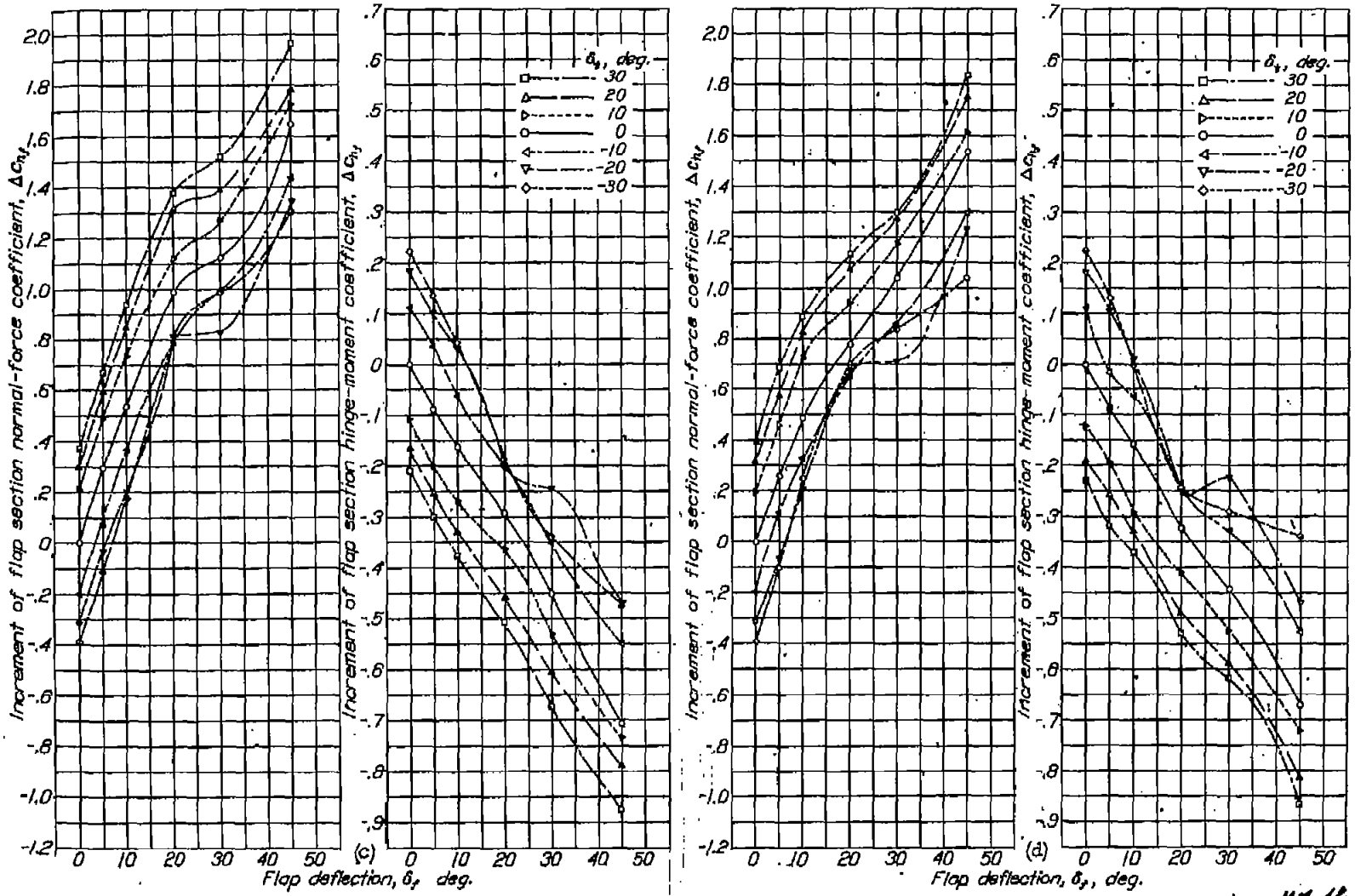

Figure 15 continued.

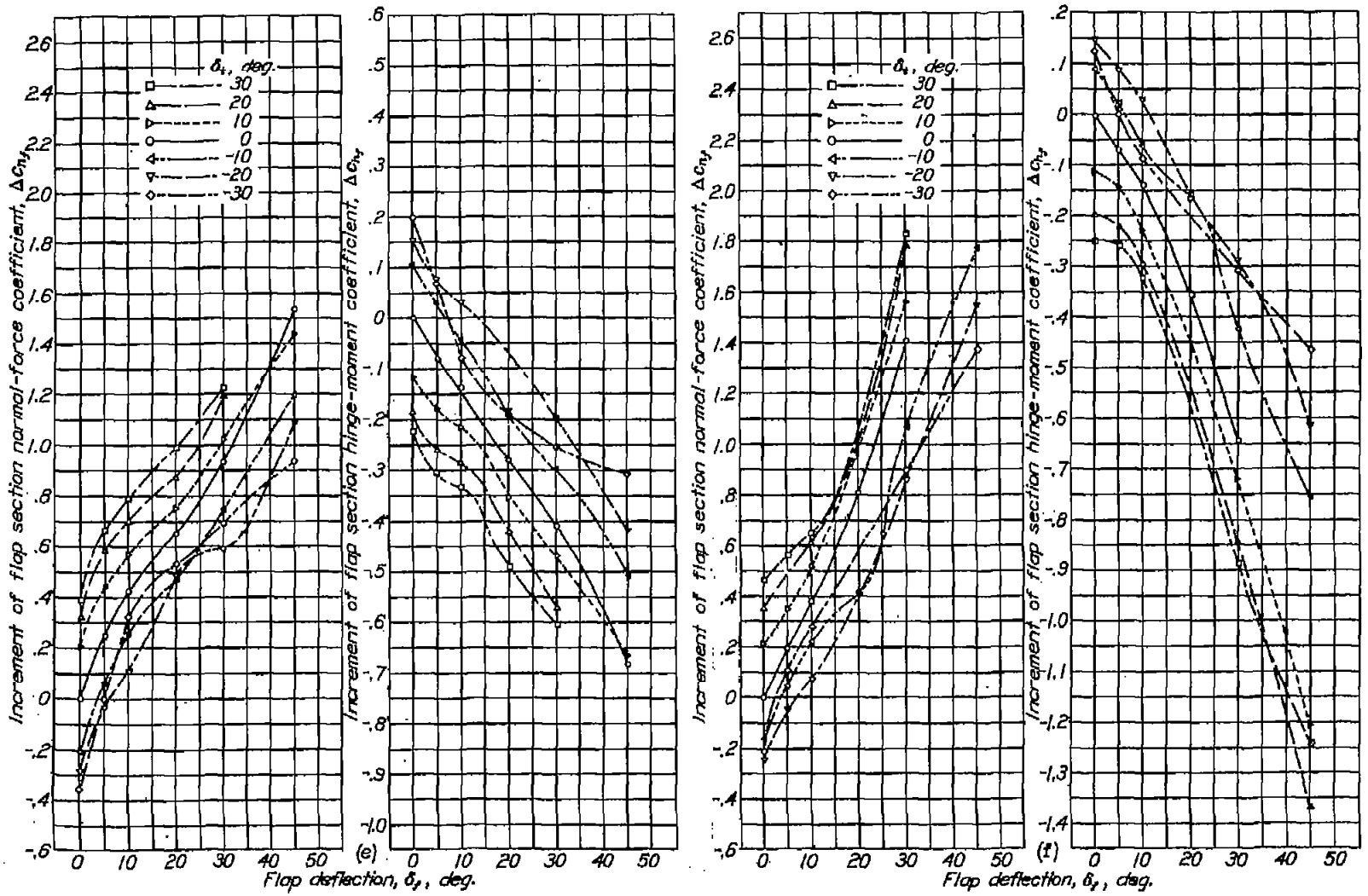

Figure 13 concluded.

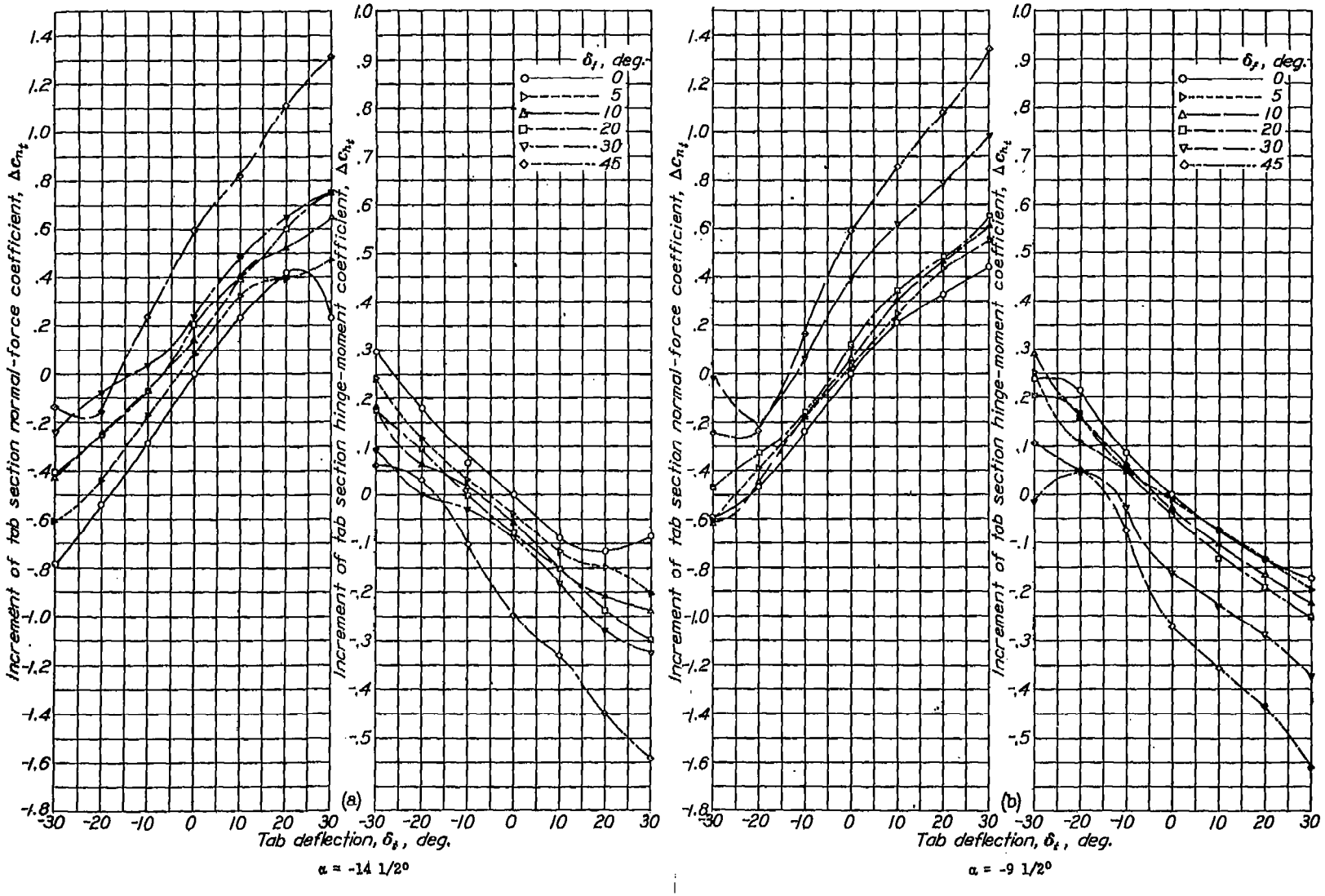

Figure 14, a to f.- Increments of tab section normal-force and hinge-moment coefficients for various deflections of a 0.50c plain flapand a $0.10c_f$ tab.

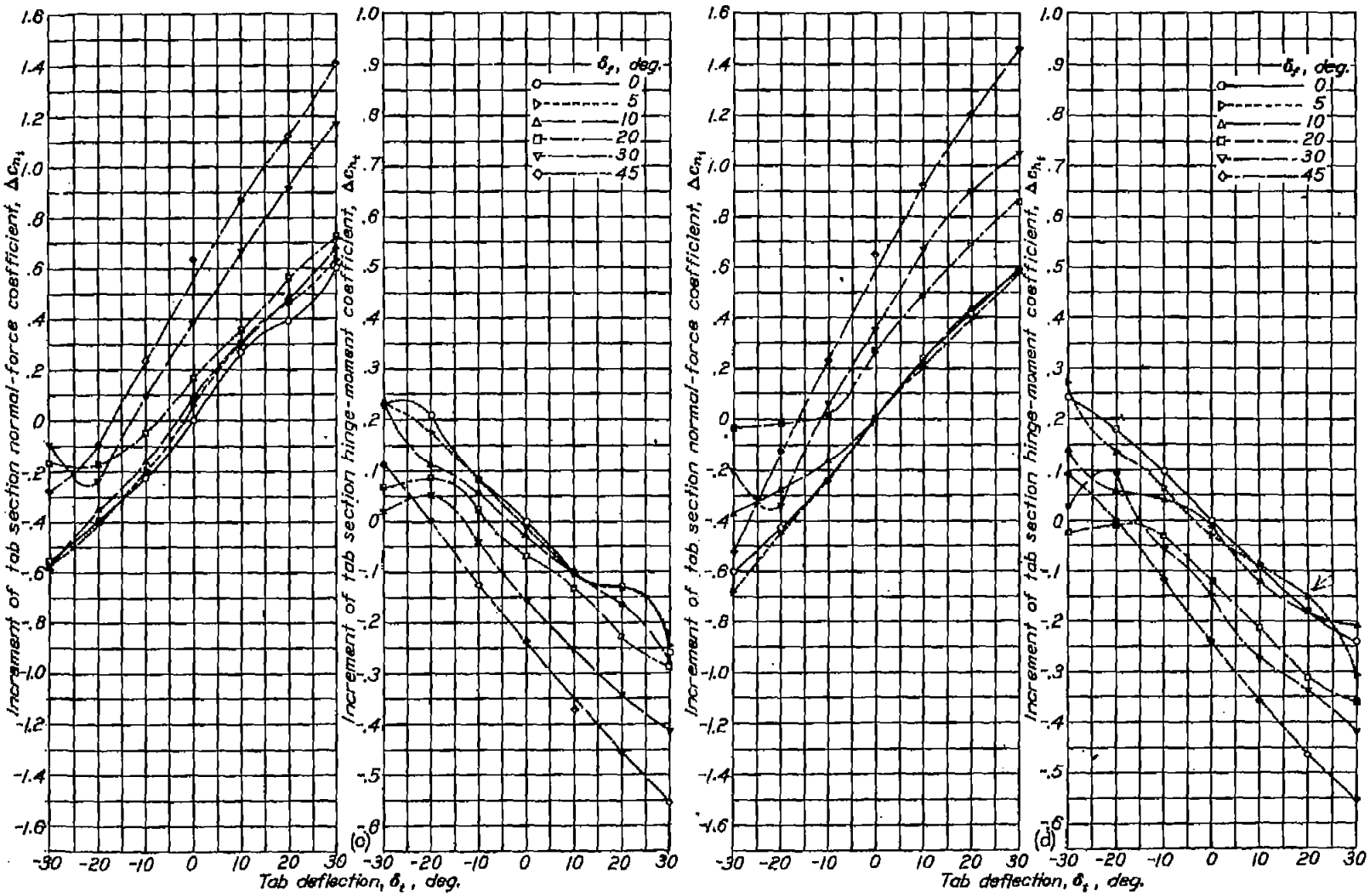

$\alpha = -4\ 1/2°$ $\alpha = 1/2°$

Figure 14 continued.

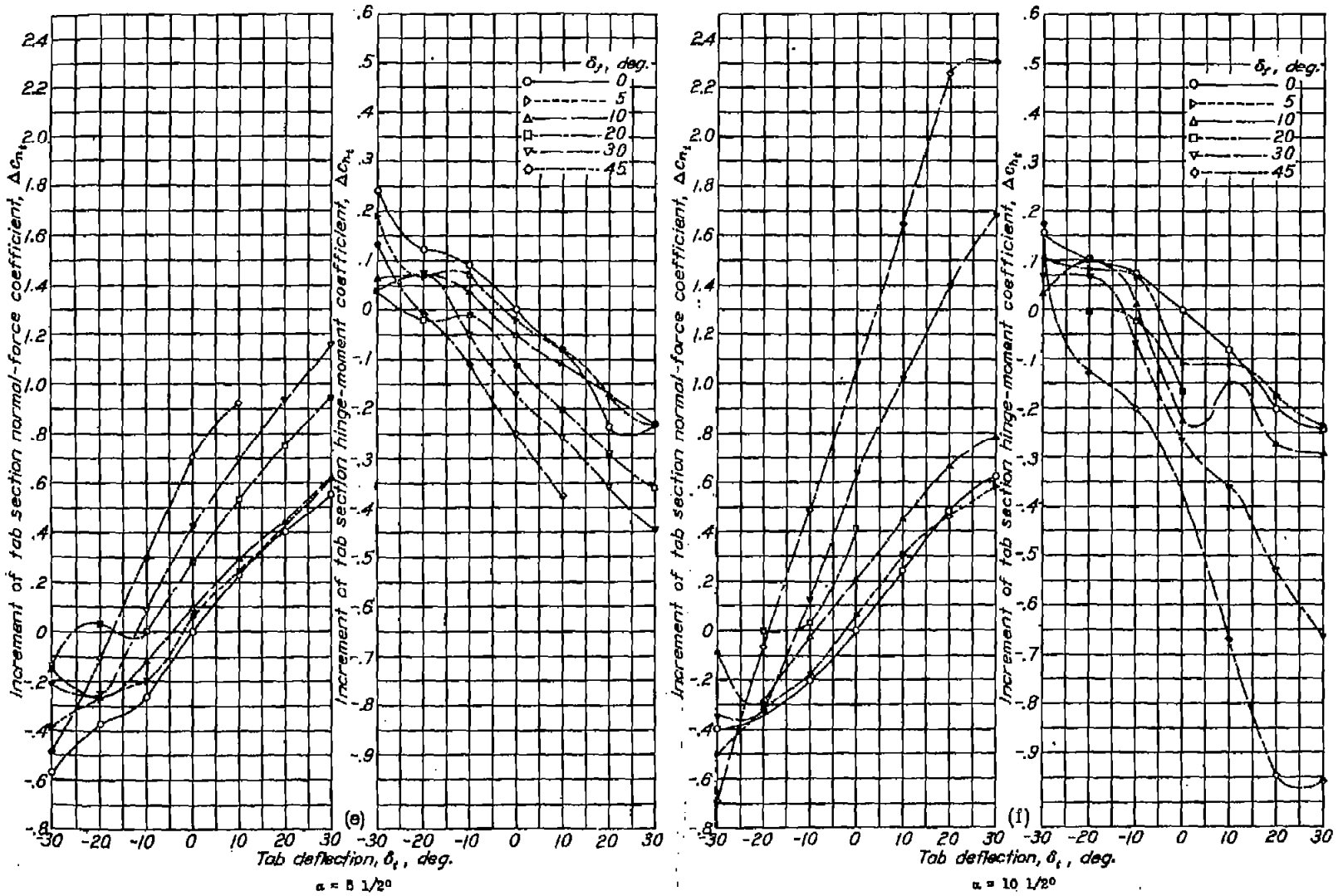

Figure 14 concluded.

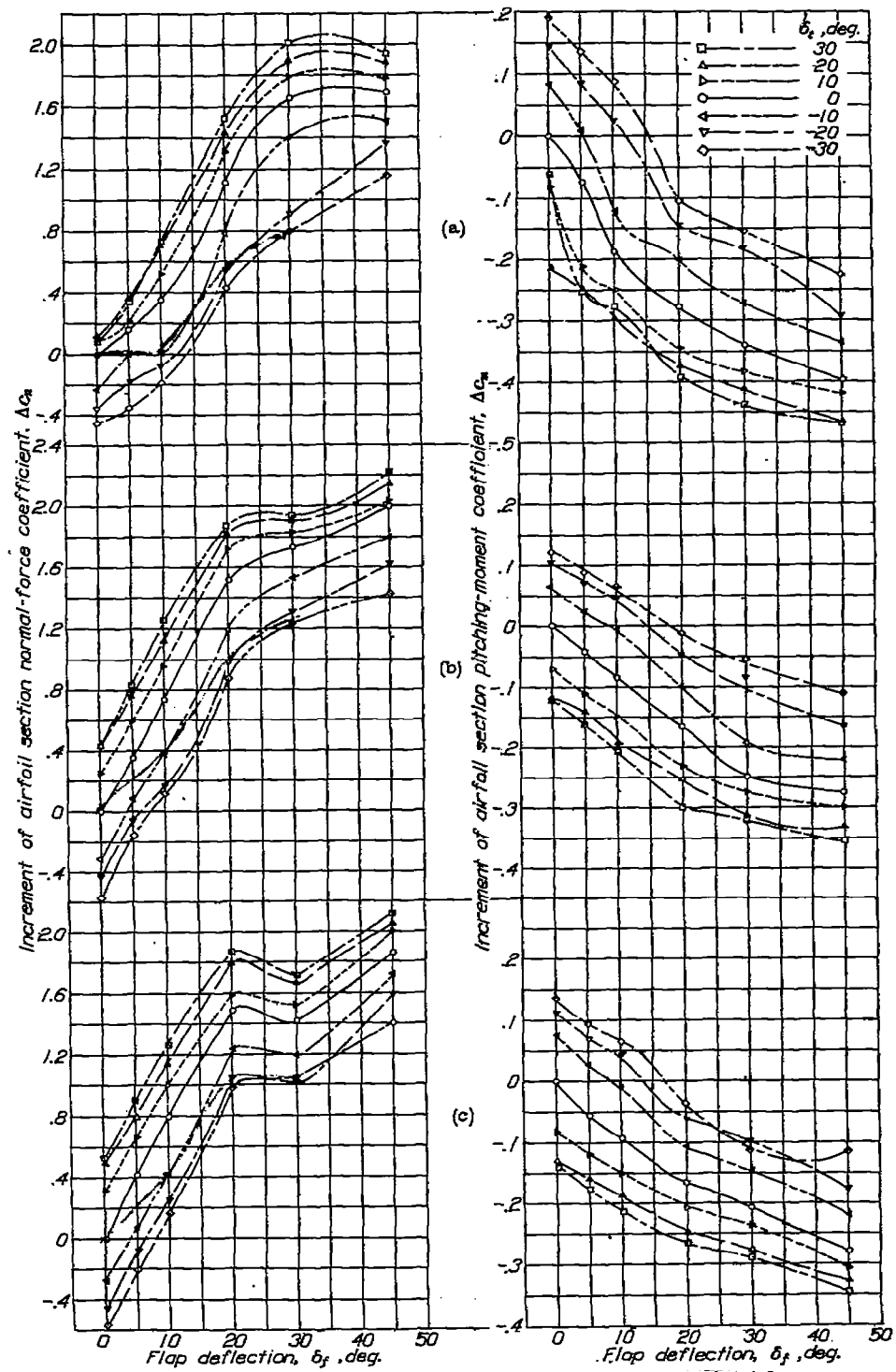

(a) α =-14 1/2° (b) α =-9 1/2° (c) α =-4 1/2°

Figure 15, a to f.- Increments of airfoil section normal-force and pitching-moment coefficients for various deflections of a 0.50c plain flap and a 0.20c_f tab.

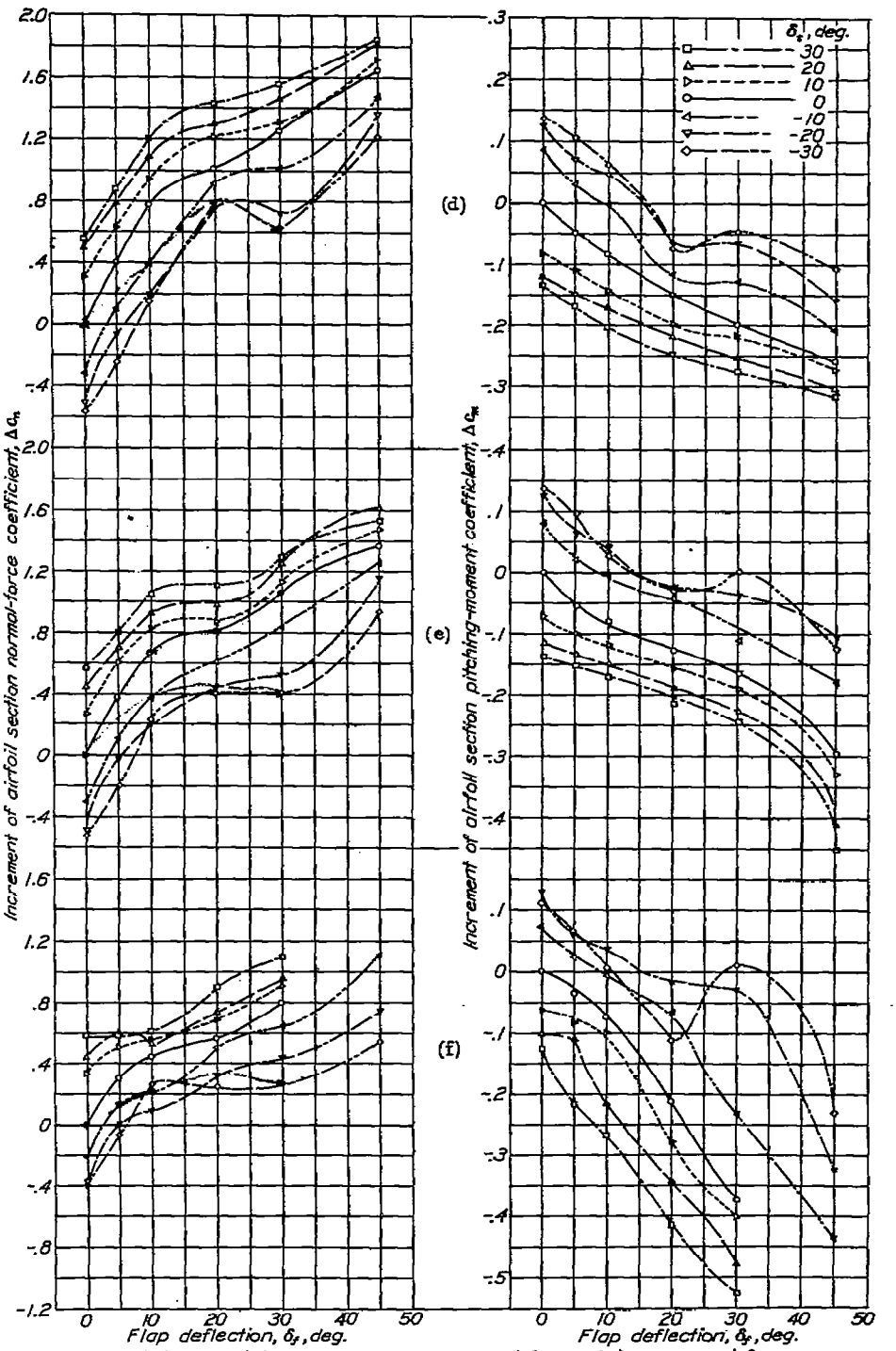

(d) $\alpha = 1/2^\circ$ (e) $\alpha = 5\ 1/2^\circ$ (f) $\alpha = 10\ 1/2^\circ$

Figure 15 concluded.

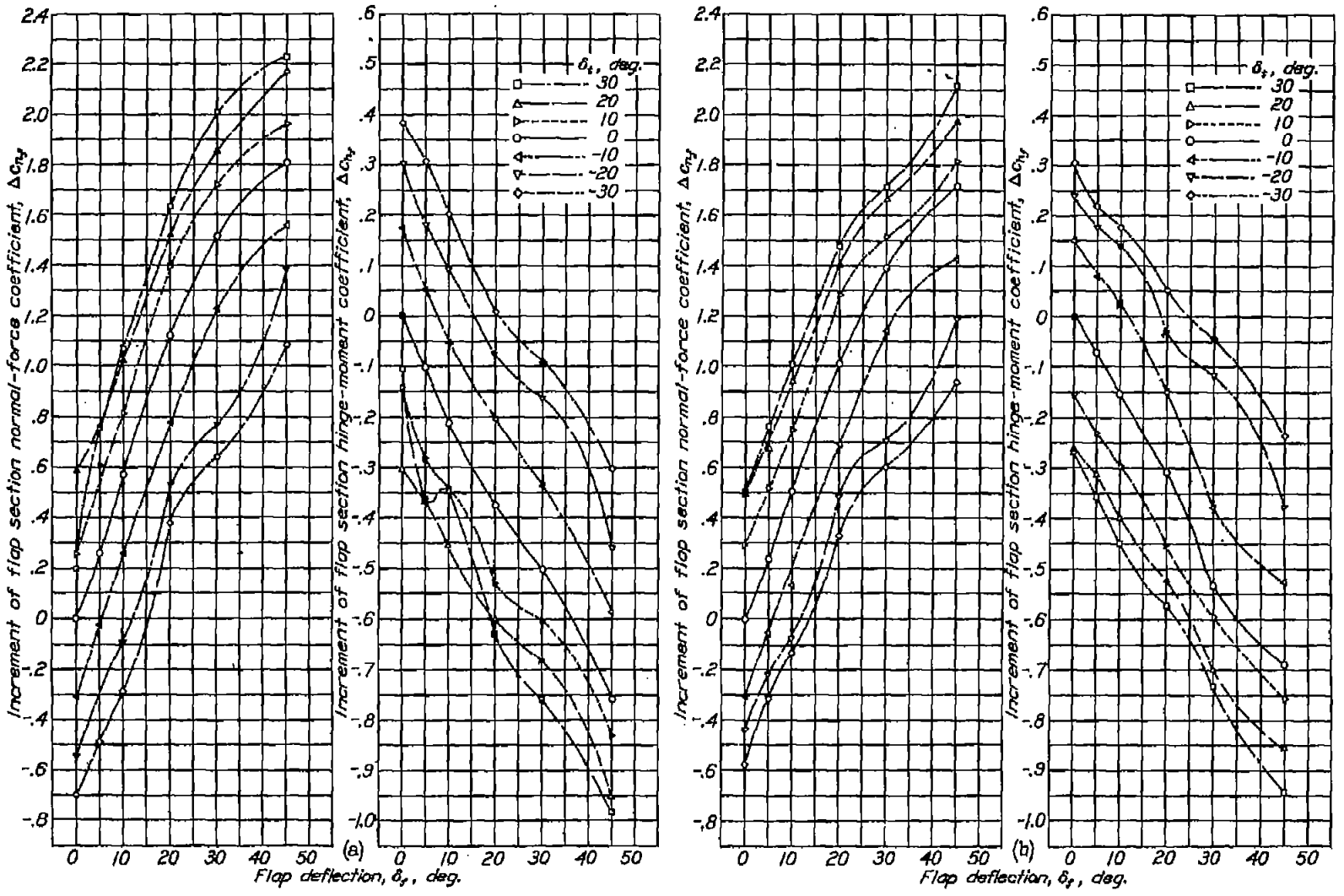

$\alpha = -14\ 1/2^\circ$ $\qquad$ $\alpha = -9\ 1/2^\circ$

Figure 16,a to f.- Increments of flap section normal-force and hinge-moment coefficients for various deflections of a 0.60c plain flap and a $0.20c_f$ tab.

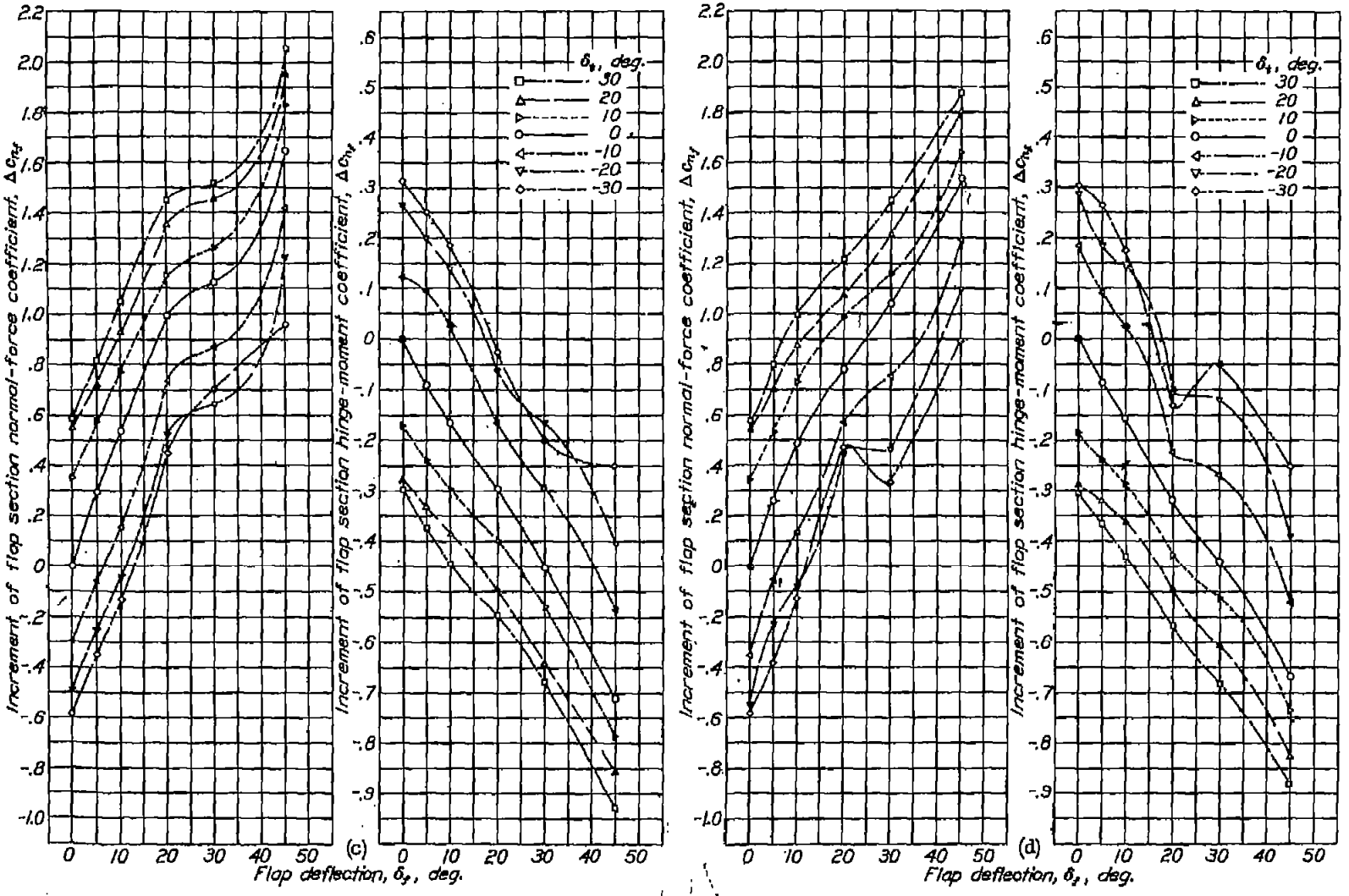

Figure 16 continued.

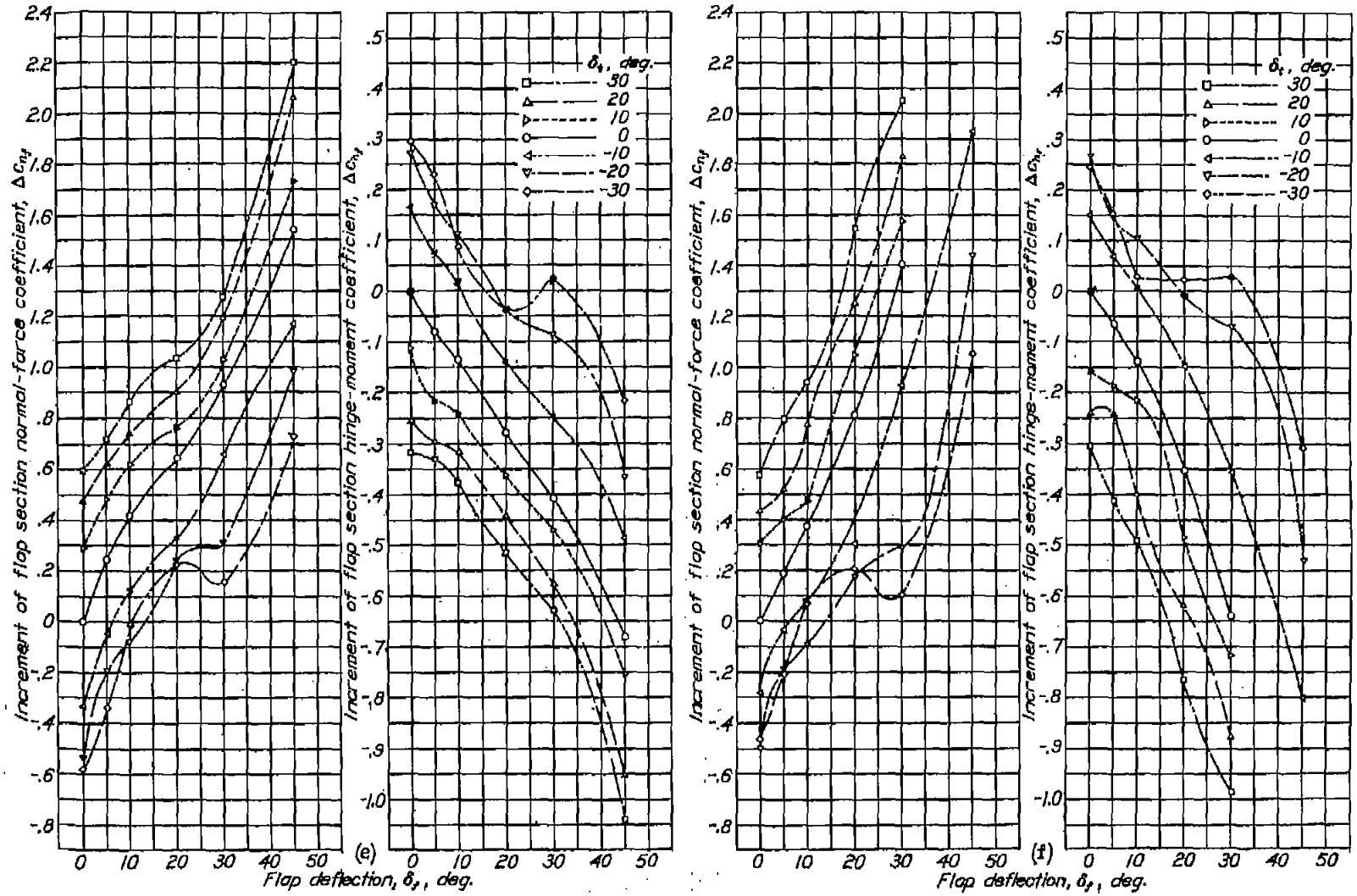

Figure 16 concluded.

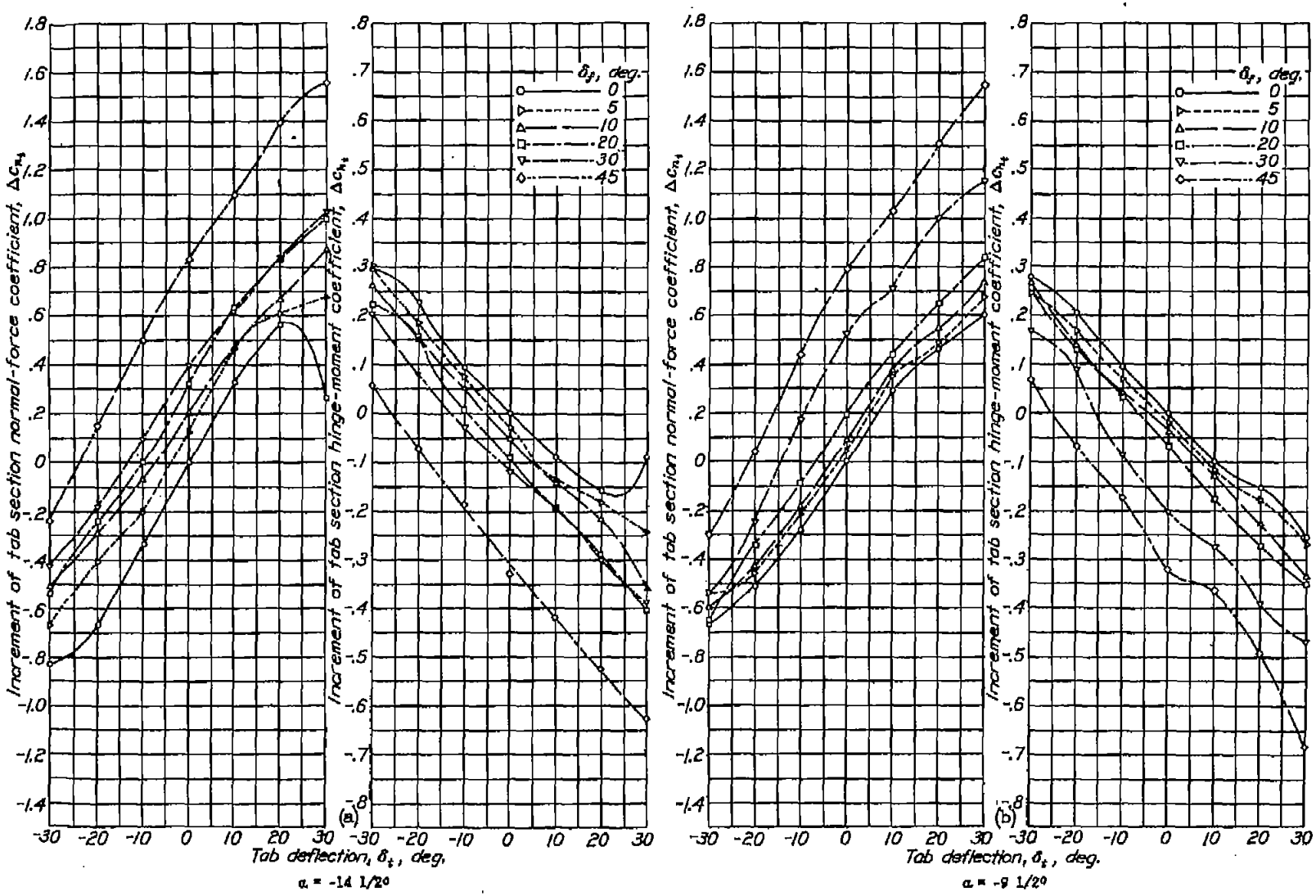

Figure 17, a to f.- Increments of tab section normal-force and hinge-moment coefficients for various deflections of a 0.60c plain flap and a 0.20c_f tab.

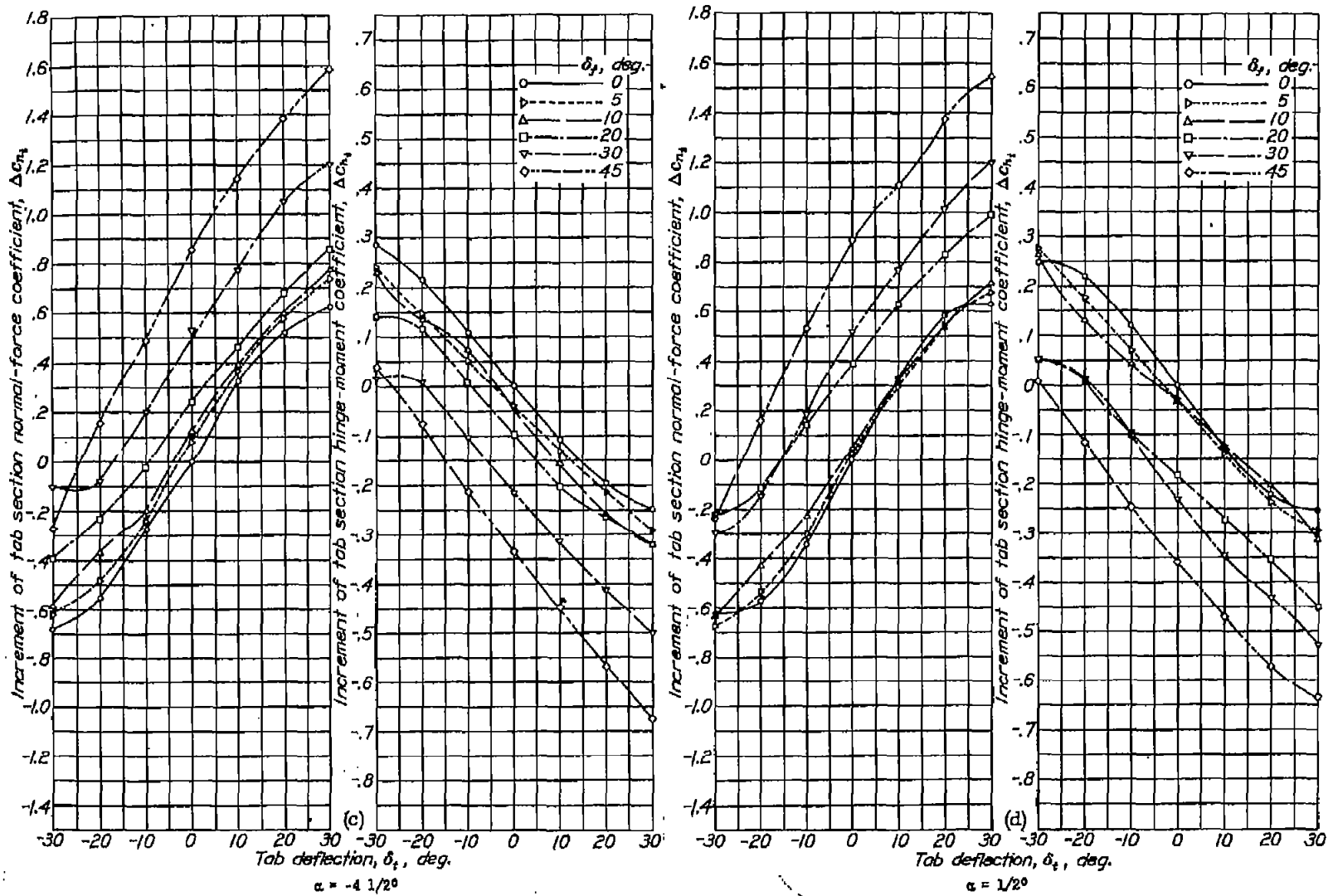

Figure 17.- continued.

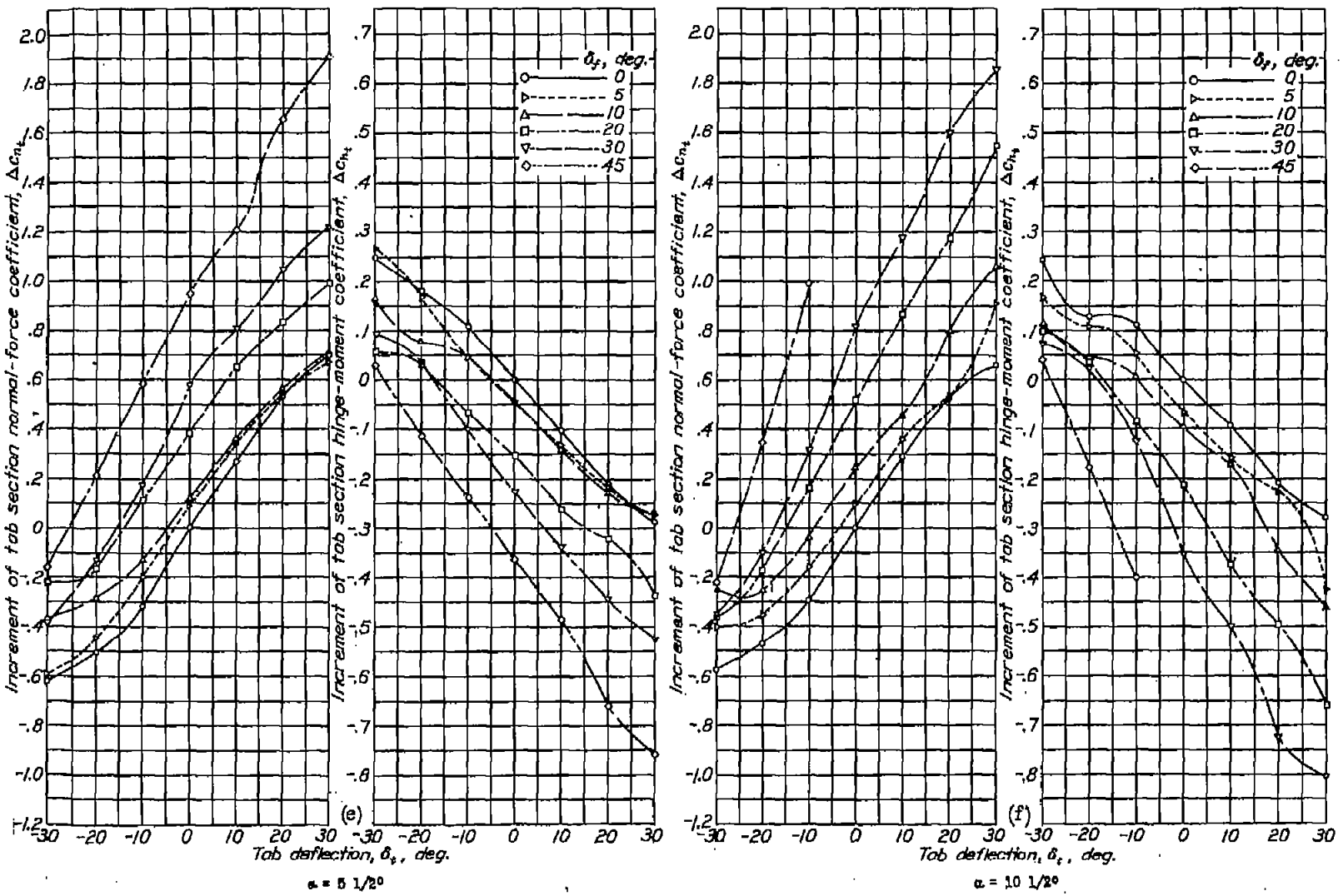

Figure 17.- concluded.

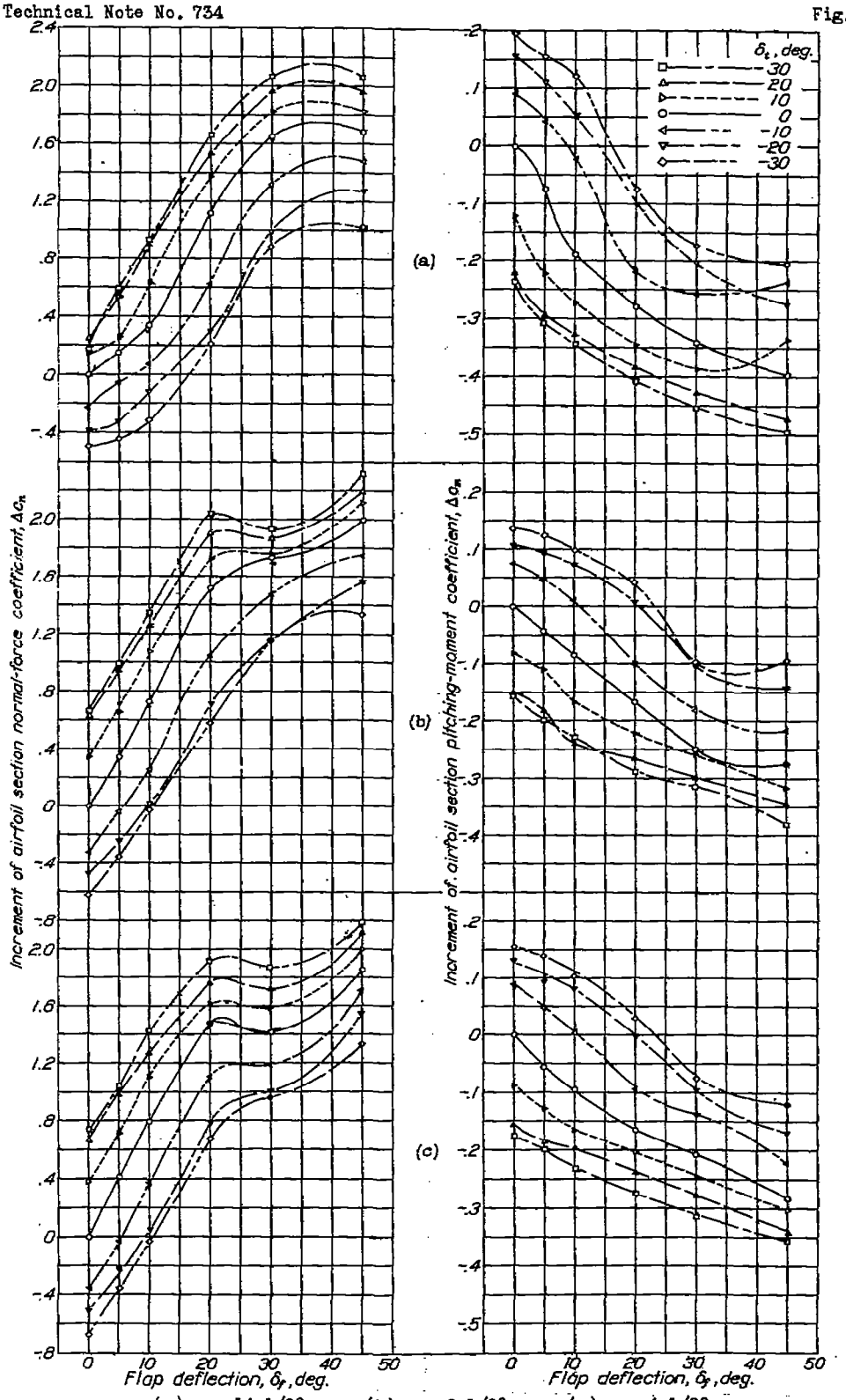

(a) α =-14 1/2° (b) α =-9 1/2° (c) α =-4 1/2°

Figure 18,a to f.- Increments of airfoil section normal-force and pitching-moment coefficients for various deflections of a 0.50c plain flap and a 0.30c_f tab.

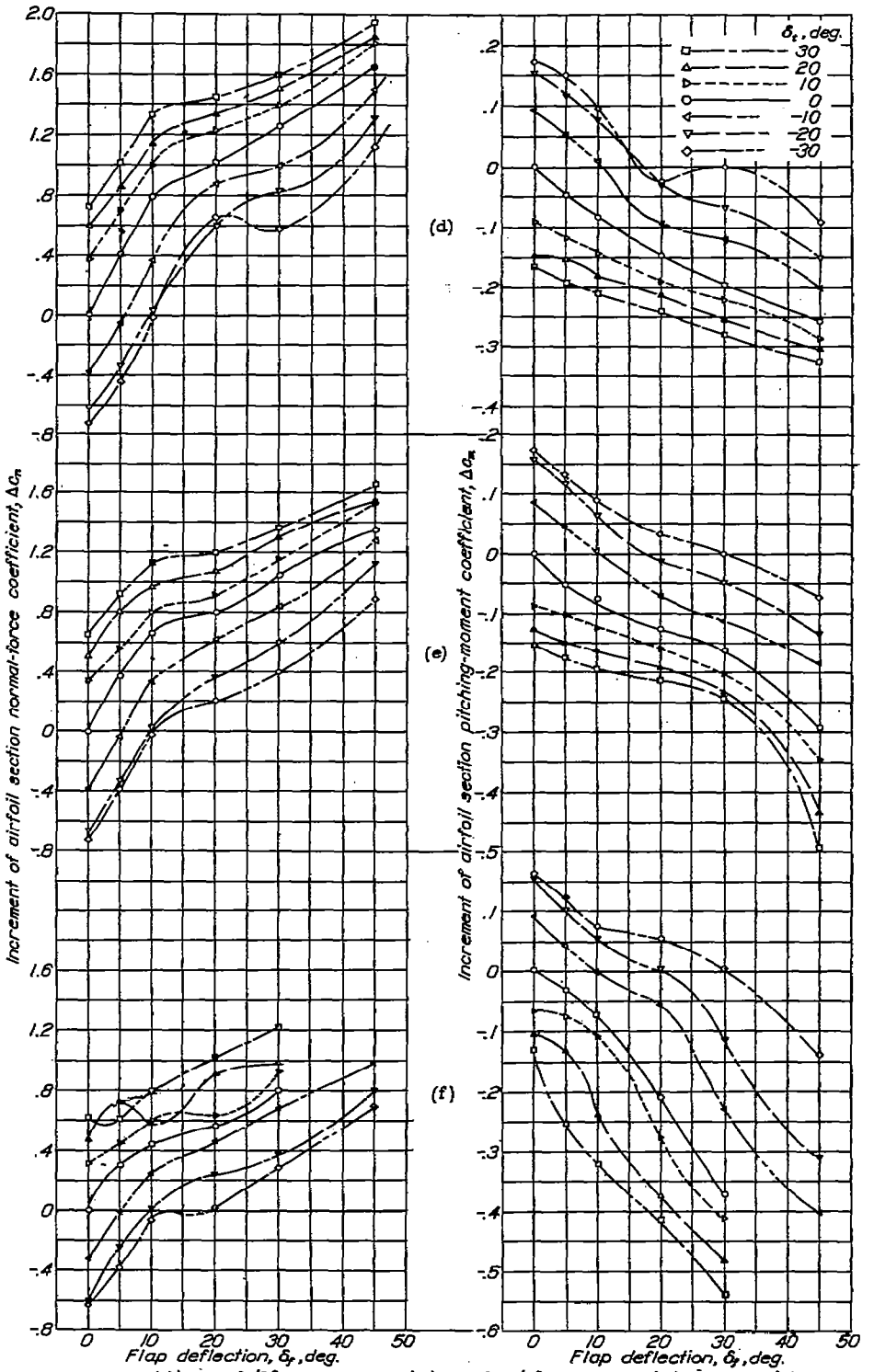

(d) α = 1/2° (e) α =5 1/2° (f) α =10 1/2°

Figure 18 concluded.

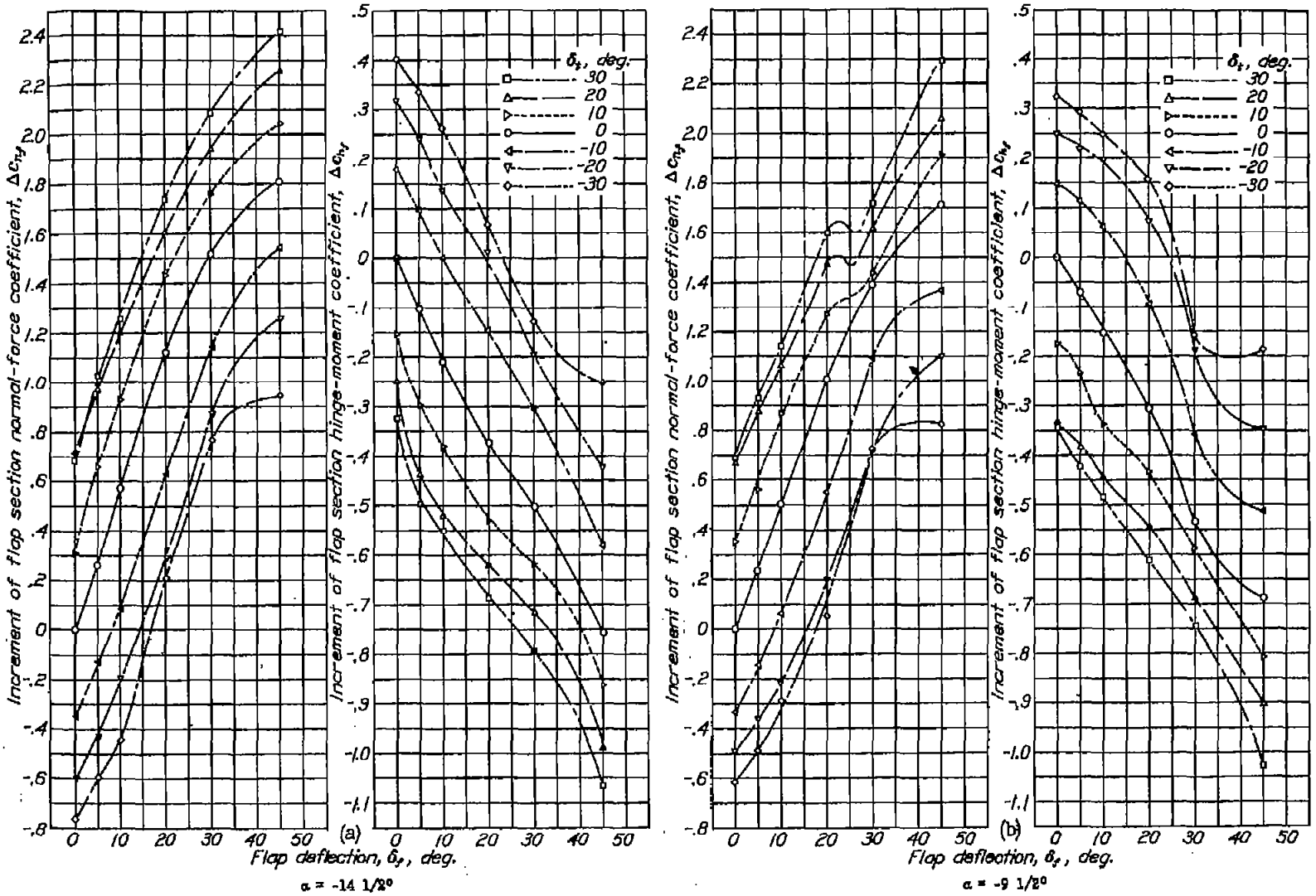

Figure 19,a to f.- Increments of flap section normal-force and hinge-moment coefficients for various deflections of a 0.50c plain flap and a $0.50c_f$ tab.

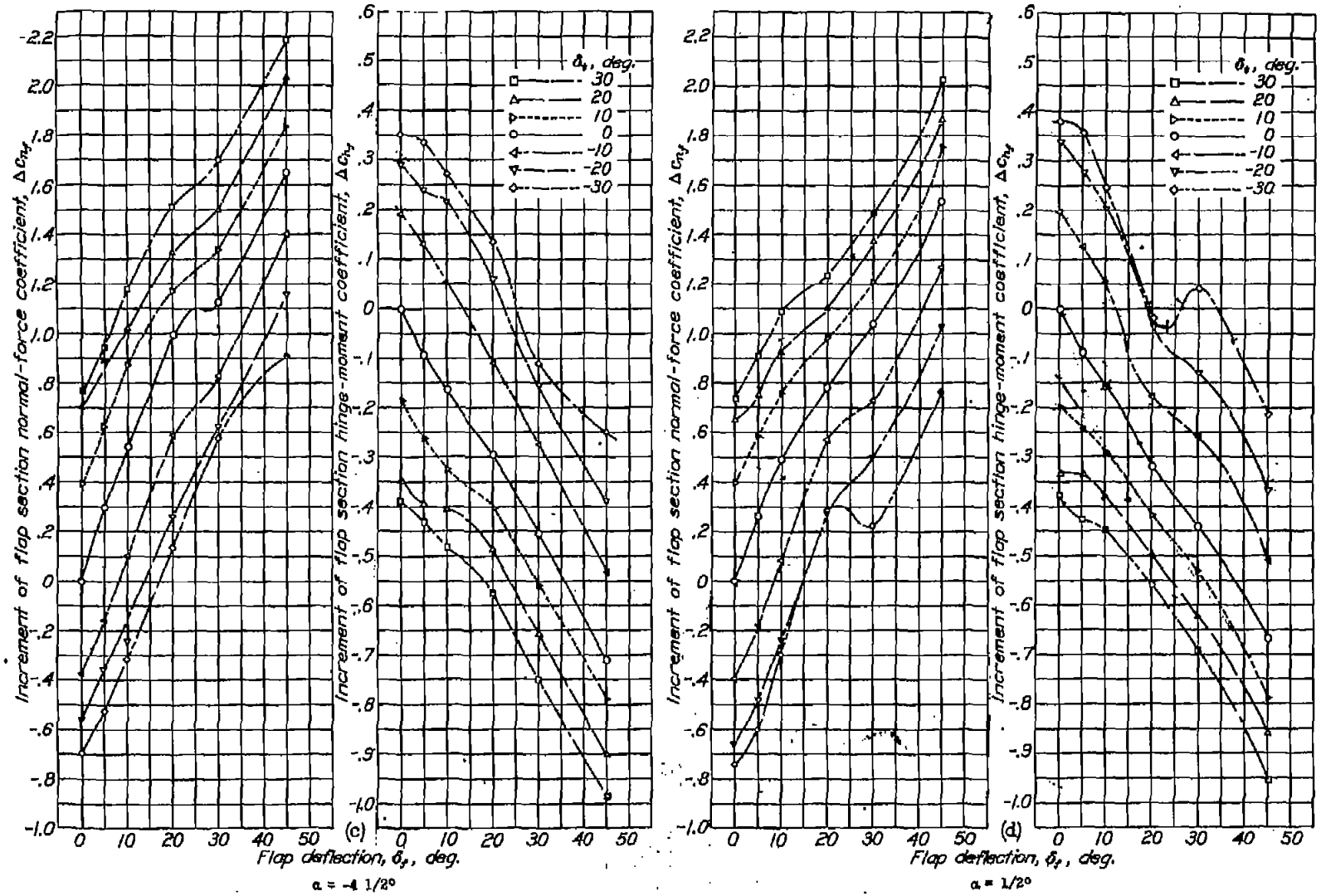

Figure 19 continued.

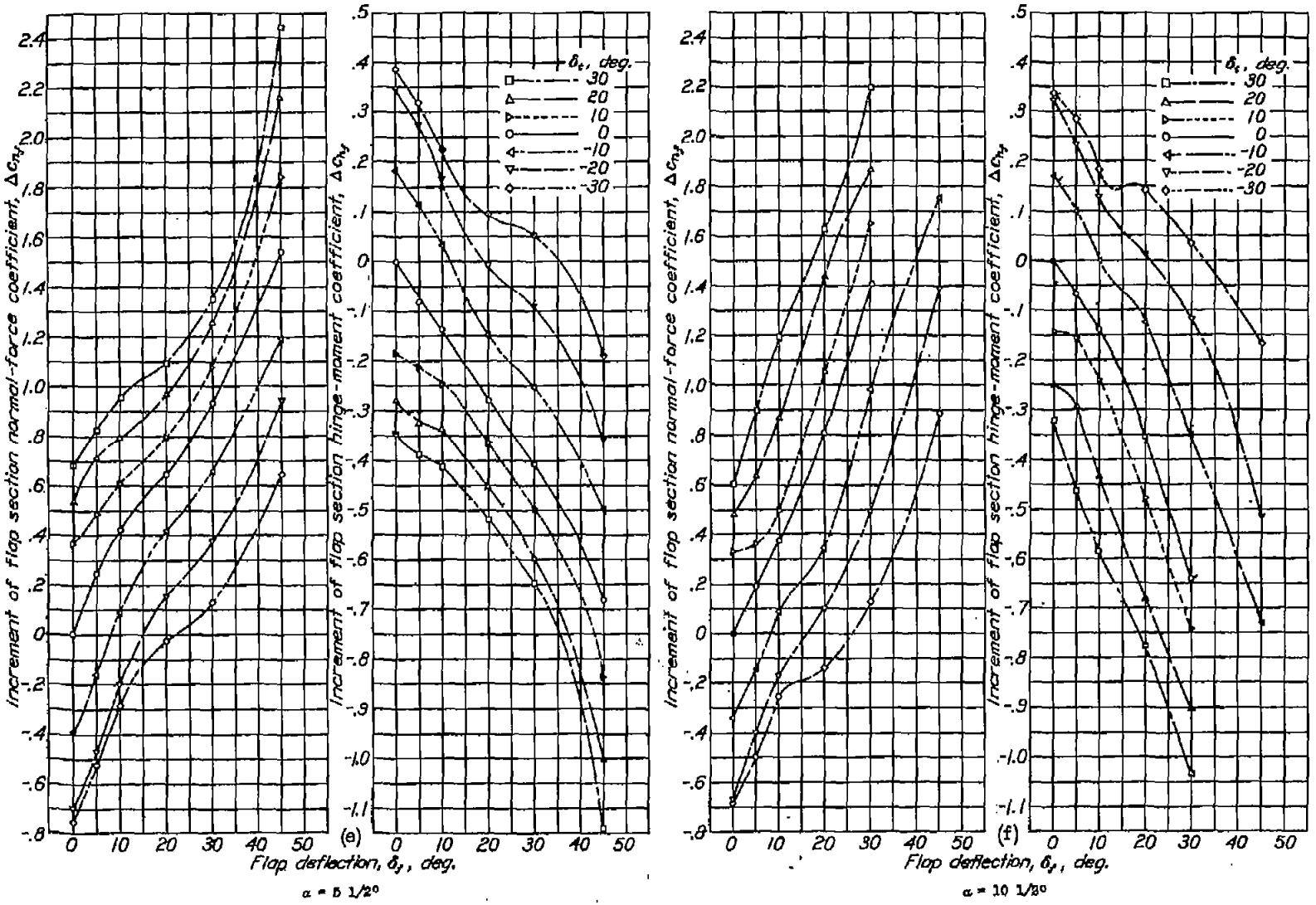

Figure 19 concluded.

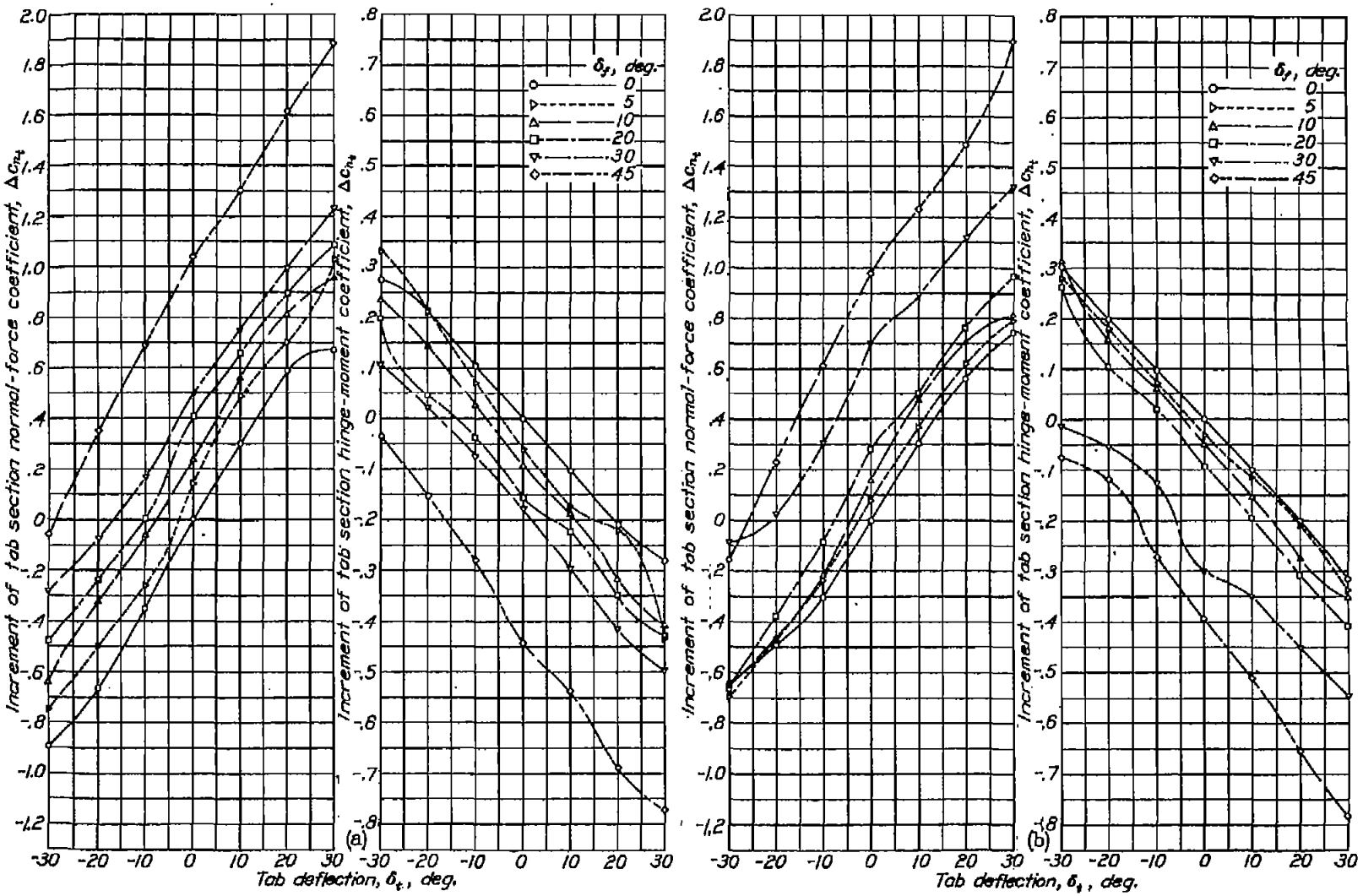

Figure 20,a to f.- Increments of tab section normal-force and hinge-moment coefficients for various deflections of a 0.50c plain flap and a $0.30c_f$ tab.

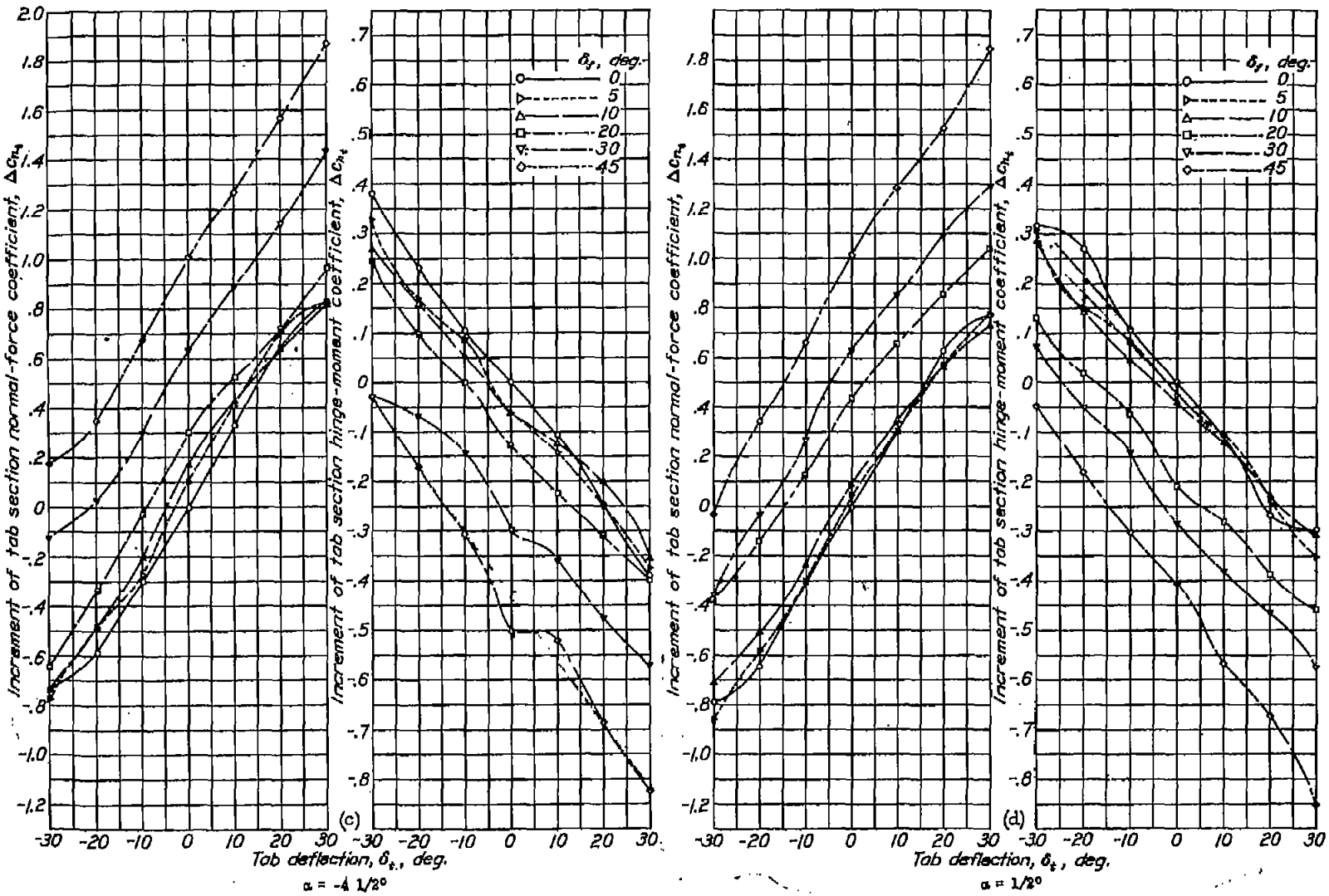

Figure 20 continued.

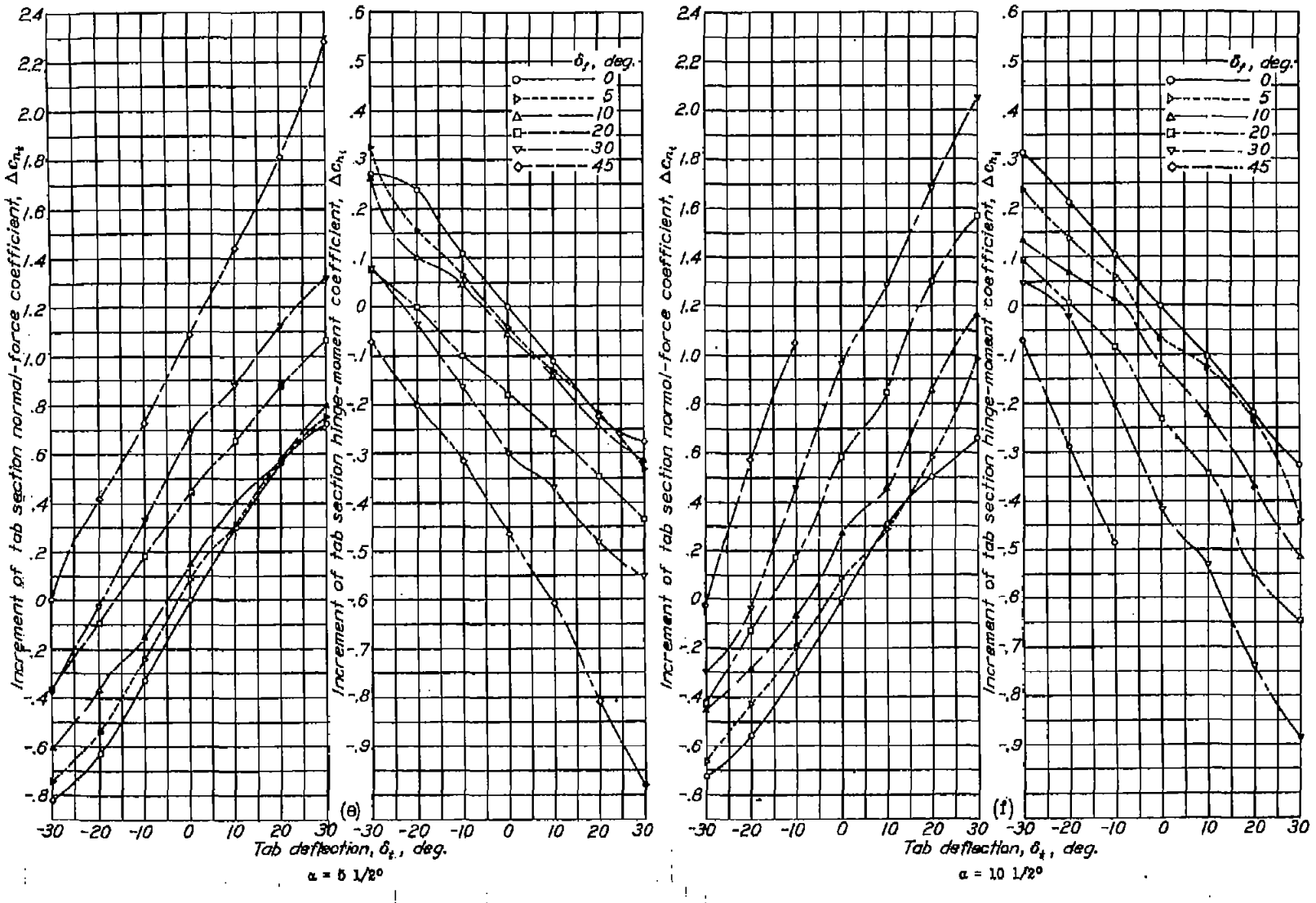

Figure 20 concluded.

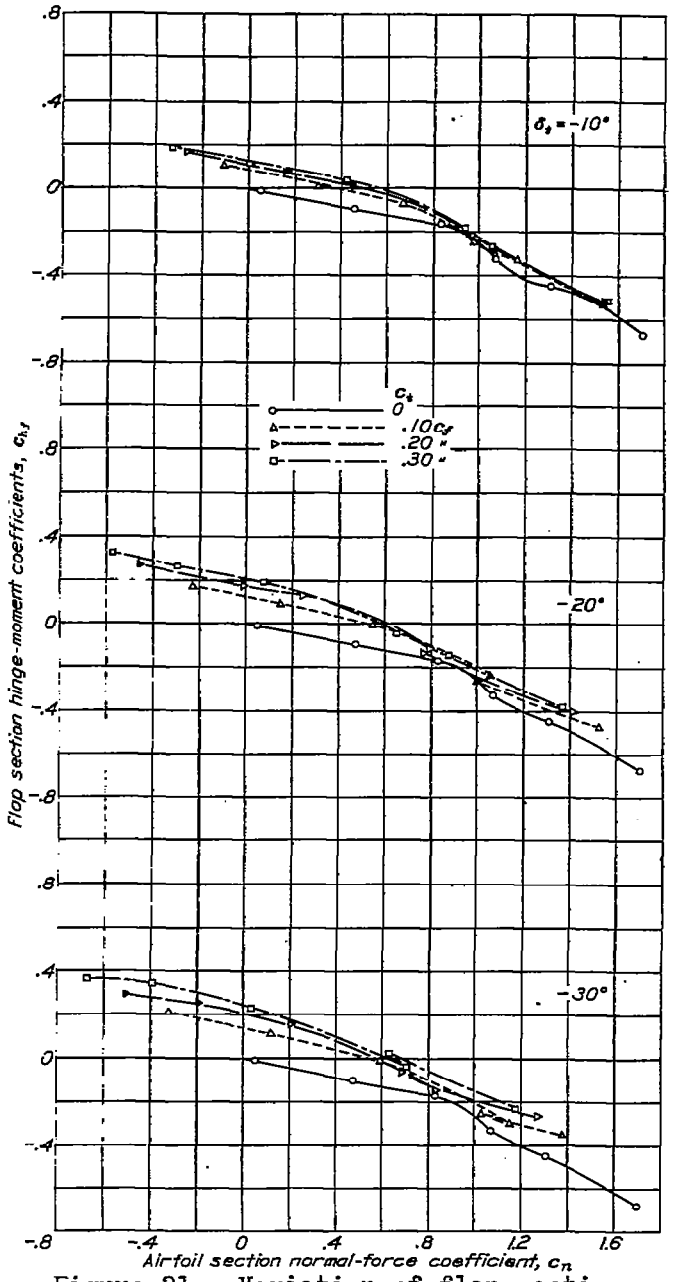

Figure 21.- Variation of flap section hinge-moment coefficient with airfoil section normal-force coefficient for various tab chords and deflections. N.A.C.A. 0009 airfoil with 0.50c plain flap, α, 1/2°.

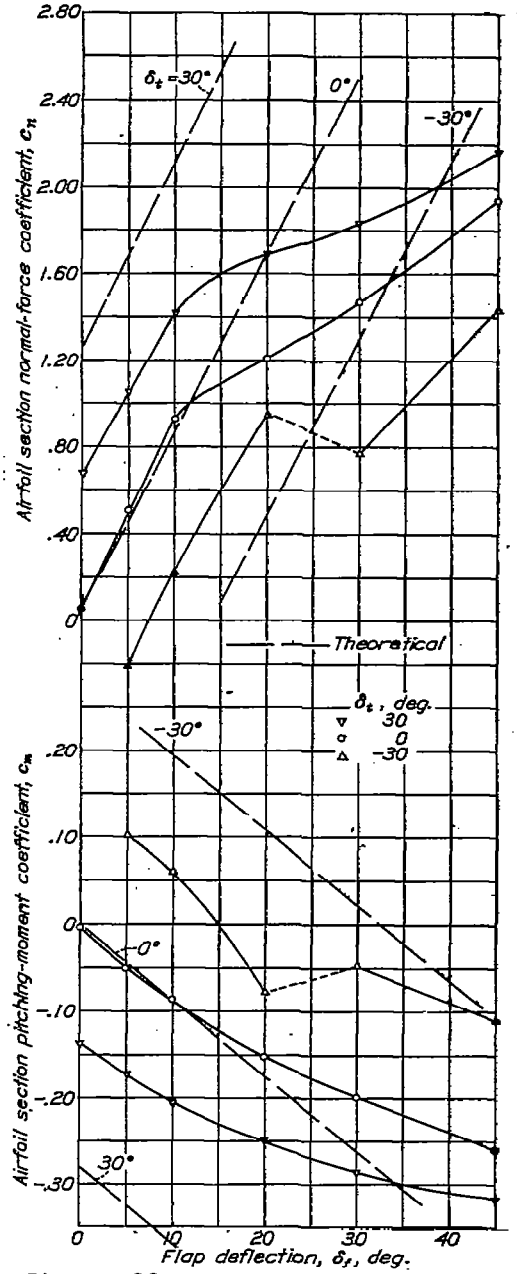

Figure 22.- Comparison of theoretical and experimental values of section normal-force and pitching-moment coefficients. N.A.C.A. 0009 airfoil with 0.50c plain flap and 0.20c_f tab, α, 1/2°.